A Tool for Preliminary Design of Rockets

Diogo Marques Gaspar

Thesis to obtain the Master of Science Degree in

Aerospace Engineering

Supervisor : Professor Paulo Jorge Soares Gil

Examination Committee

Chairperson:	Professor Fernando José Parracho Lau
Supervisor:	Professor Paulo Jorge Soares Gil
Members of the Committee:	Professor João Manuel Gonçalves de Sousa Oliveira

July 2014

Dedicated to my Mother

Acknowledgments

To my supervisor Professor Paulo Gil for the opportunity to work on this interesting subject and for all his support and patience.

To my family, in particular to my parents and brothers for all the support and affection since ever.

To my friends: from IST for all the companionship in all this years and from Coimbra for the fellowship since I remember.

To my teammates for all the victories and good moments.

Resumo

A única forma que a humanidade até agora conseguiu encontrar para explorar o espaço é através do uso de rockets, vulgarmente conhecidos como foguetões, responsáveis por transportar cargas da Terra para o Espaço.

O principal objectivo no design de rockets é diminuir o peso na descolagem e maximizar o payload ratio i.e. aumentar a capacidade de carga útil ao seu alcance. A latitude e o local de lançamento, a órbita desejada, as características de propulsão e estruturais são constrangimentos ao projecto do foguetão.

As trajectórias dos foguetões estão permanentemente a ser optimizadas, devido a necessidade de aumento da carga útil transportada e redução do combustível consumido. É um processo utilizado nas fases iniciais do design de uma missão, que afecta partes cruciais do planeamento, desde a concepção do veículo até aos seus objectivos globais.

O principal objectivo deste trabalho é encontrar o design mais adequado de um foguetão, para uma órbita e carga específicas, considerando a melhor trajectória que pode ser utilizada. Foi desenvolvido um programa que permite o estudo de diferentes configurações e a variação dos parâmetros de design, calculando para cada configuração e conjunto de parâmetros as diferentes massas e dimensões do foguetão, para depois iterativamente com a trajectória conseguir maximizar o payload ratio, minimizando o peso na descolagem. Para validar o código foram feitas comparações com os resultados obtidos para os lançadores Vega e Proton K/DM3. Por último, é feita uma optimização do lançador Ariane 5 através da variação da sua configuração e de parâmetros de design.

Palavras-chave: Multi-Estágios Rockets, Gravity Turn, Optimização de Trajectória, Optimização de Rockets, Maximizar o Payload Ratio.

Abstract

The only way mankind can explore space is with the use of space launch vehicles, commonly known as rockets, which carry payloads from Earth into Space.

The main goal in the rocket design is to reduce the gross lift-off weight (GLOW) and increase the payload ratio, giving them the capacity of having the maximum amount of payload or its range. Launch latitude, launch site, final kick-off location for payload, propulsion characteristics and, or, its own structural characteristics are all limitations in the launch vehicle's design.

The trajectories of launch vehicles are permanently being optimized, due to the demand of increased payload and reduced propellant requirements. Optimization of a trajectory is a process used in early stages of the mission design, it affects crucial parts of mission planning, ranging from vehicle design to even overall mission objectives.

The main objective of this study is to find the best design of a rocket for a specific orbit and payload mass, considering the best trajectory that can be used. A tool was developed allowing the study of different configurations and the variation of design parameters, calculating for each configuration and parameters the different masses and dimensions that characterize a rocket, and then iteratively with the trajectory will achieve the minimum GLOW and obtain the maximum payload ratio. In order to validate the code comparisons with Vega and Proton K/DM3 launchers were made. At last an optimization of the Ariane 5 launcher is made by varying its configuration and some design parameters.

Keywords: Multistage Rockets, Gravity Turn, Trajectory optimization, Rocket optimization, Maximize Payload Ratio.

Contents

List of Tables

List of Figures

Nomenclature

$\dot{m}$	Mass Flow Rate.
m_{fair}	Fairing Mass.
m_{fuel}	Fuel Mass.
m_{ox}	Oxidizer Mass.
m_o	Rocket Section Mass.
ΔV	Delta-V.
$\frac{T}{W}$	Thrust to Weight Ratio.
C_D	Coefficient of drag.
I_{sp}	Specific Impulse.
m_{pay}	Payload Mass.
m_p	Propellant Mass.
m_s	Structural Mass.
P_{amb}	Ambient pressure.
P_e	Pressure at exit.
V_{circ}	Velocity - Circular Orbit.
V_e	Exhaust velocity.
V_{fuel}	Volume of fuel Tank.
V_{ox}	Volume of oxidizer Tank.
V_{tank}	Volume of Tank.

Greek symbols

α	Angle of attack.
γ	Flight Path Angle.

λ Payload Ratio.

Λ Mass Ratio.

μ gravitational parameter.

ρ Air Density.

ε Structural Ratio.

Roman symbols

bt Burning Time.

D Drag.

g gravitational acceleration.

g_0 gravitational acceleration at sea level.

H Altitude.

p Pressure.

S Surface Area.

T Thrust.

th thickness.

X Downrange.

Glossary

AP	Ammonium Perchlorate
DB	Double Base
ESA	European Space Agency
F2	Liquid Fluorine
GEO	Geosynchronous Earth Orbit
GLOW	Gross Lift Off Weight
GTO	Geostationary Transfer Orbit
GT	Gravity Turn
H-2	Liquid Hydrogen
HMX	Cyclo-tetramethylene tetranitramine
HTPB	Hydroxyl-terminated polybutadiene
LEO	Low Earth Orbit
LOX	Liquid Oxygen
LVD	Launch Vehicle Design
MDO	Multi-Disciplinary Optimization
MER	Mass Estimation Relationship
MMH	Monomethylhydrazine
MR	Mixture Ratio
OF	Oxidizer to Fuel Ratio
RLV	Reusable Launch Vehicle
RP-1	Refined Petroleum 1
TPBVP	Two Point Boundary Value Problem
UDMH	Unsymmetrical dimethylhydrazine

Chapter 1

Introduction

1.1 Goal of this work

The objective of this work is to develop a tool that will help design a multistage rocket, by obtaining an preliminary sizing of the rocket and access the possible design trade-offs in order to maximize its performance under some criteria.

1.2 History of Rockets

Modern rockets are the result of more than two thousand years of experiences, failures and inventions. The first reported device to use rocket propulsion was developed in the 4th century b.C. in Greece, by Archytas, who constructs and flies a small device, propelled by a jet of steam or compressed air. Later on in the 13th century, during the war between China and Mongolia, the Chinese troops developed a mixture of saltpeter, sulfur, and charcoal dust that produces colourful sparks and smoke, when ignited. This powder was used to make fireworks, giving birth to the first concept of rocketry [6, 7].

In the beginning of the 17th century, Kasimierz Siemienowicz, commander of the Polish Royal Artillery, writes a manuscript on rocketry, *Artis Magnae Artilleriae pars prima*, which includes a design for multistage rockets, essential technology for spaceflight rockets. Well-known scientists, Galileo Galilei and Isaac Newton, 15th and 17th century respectively, develop the fundamental theories in the field of physics, with their works in motion, particularly Newton's Laws of Motion published in *Philosophiae Naturalis Principia Mathematica* provides the foundation for all modern rocket science. Konstantin E. Tsiolkovski known for his rocket equation, based on Newton's second law of motion, and his work - *Research into Interplanetary Space by Means of Rocket Power*, published in 1903, was an astronautics pioneer, considered the father of cosmonautics and spaceflight. A few years later, in 1926, an American college professor and scientist, Robert H. Goddard, known as the father of modern rocketry in the US, builds and flies the world's first liquid propellant rocket, essential to be able to reach space [6].

In the 1920s and 1930s, before World War II, scientists and amateur rocketeers attempted to use rockets in every mean of transport, and though there were numerous failures, the experiments allowed

to improve rockets, making them more powerful and reliable. During World War II, the Germans built and flew the most advanced rocket developed till then, the V2. The space era began in 1957 when the Soviet Union amazed the world when it launched the world's first artificial satellite, Sputnik 1. Less than a month later, the Soviets followed with the launch of a satellite carrying a dog named Laika on board. The great mind behind the V2 project was Dr. Wernher von Braun that led the development team that launched Explorer 1 in 1958 by USA, and was also chief architect and engineer of the Saturn V Moon Rocket. In 1961 Vostok 1 carried the first human into outer space cosmonaut Yuri Gagarin [8].

In the same year Freedom 7, launched by the US, makes a suborbital flight, because the rocket didn't have enough power to send the spacecraft to orbit. Until 1966 ten Gemini missions reached orbit, with the help of a Titan missile. The Saturn V appears in the late sixties, capable of launching up to 118 tons into Low Earth Orbit (LEO) and 41 tons to the Moon. After the end of Apollo program the investment decreases, but new families of rockets appear. Delta family is one of the most versatile payload launch rocket, with many configurations including multiple stages and heavy-lift-strap-on boosters that increase payload capacity to high orbits [9].

In USSR several launchers have been designed and launched, the most relevant is Proton who started is mission in 1965 and is still in active, recognized as a commercial workhorse of the Russian space program. After launching the service module of the International Space Station in 2000, the four-stage version of Proton launched numerous satellites for the Russian government and foreign customers [6]. In 1975, European Space Agency (ESA) was created in Europe, rapidly starts with the development of the Ariane family. ESA's primary launcher is Ariane 5, in service since 1997, capable of delivering between 6 to 10 tons into GTO and 21 tons into LEO.

In 1981 takes place the first flight of a Space Shuttle, by the US, carrying a crew and payloads, into LEO, it's presented in the figure 1.1. Russia tries to do the same by designing Buran, but it turns out to be a disaster, because it only flies two times. Nowadays the essential to NASA's plans is a new and versatile space launch system, to replace the space shuttle. The constellation program that separates human crews and payloads, for safety, is expected to combine the best of the past National Aeronautics and Space Administration (NASA) decades of experience, with the best of present and future. Where Ares I is a Crew Launch Vehicle, a two stage rocket with a crew capsule on top and Ares V will become NASA's primary heavy-lift cargo launch vehicle. ESA also developed Vega, for small payloads, capable of placing multiple payloads into orbit. In cooperation with Russia, ESA allowed the launch of Soyuz-2 from French Guiana, capable of delivering 3 tons into GTO. Other countries, such as India, Japan and China, although in a smaller scale, developed their own space programs. In China, Long March family was the best know launcher, capable of delivering 12 tons into LEO. In Japan H-IIA was used to deliver 6 tons into GTO, and recently, H-IIB was developed, capable of delivering up to 8 tons into GTO. Launched from an aircraft Pegasus is lifted to about 12 km and then, air launched from under the aircraft. This special arrangement was developed to keep launch costs low for small orbital payloads [9].

Figure 1.1: Space Shuttle [2]

1.3 Challenges in the design of a Rocket

Although the first spaceflight took place more than fifty years ago, currently we depend on very expensive vehicles and only some are reusable. Besides, for a conventional launch vehicle to reach orbit, the velocity required is so high that it has to be composed of two or more separated vehicles, mounted on top of each other and the payload is only a small part of the total vehicle mass. Since the 1950s that launch vehicles have almost the same shape and use almost the same propellants, like the Atlas, Delta and Titan, which are upgraded versions of the first designs, showing not much progress in the conceptual design of launch vehicles [2, 10].

The preliminary design and optimization of rockets has been the focus of several research studies. The minimum GLOW can be obtained by staging and trajectory optimization [11, 12]. The collaborative optimization is an alternative design architecture, whose characteristics are well suited for launch vehicle design [13]. The Multidisciplinary Optimization (MDO) strategies are based in the exploration on the interaction of sub-systems representative models and on the exploitation of their coupling, in order to find the optimal conception parameters. Several works using MDO have been developed in the preliminary design and optimization of rockets [14, 15, 16, 17, 18]. Recently, one work in multi-attribute evaluation provided an interesting approach in the conceptual design of rockets with a cost model [19].

One of the main issues in the design of Launchers is how to reduce their structural mass. The improvements done in composite structures allow lightweight structures, but their reliability has not yet

been proven. Liquid or hybrid propellants are used in upper stages, since they allow engine restart and accurate orbit insertion [2]. Solid stages for boosters are usually cheaper to design, test, and produce, compared to equivalent liquid or hybrid boosters, and don't involve refrigeration requirements [20]. Minimizing g-forces, for the comfort of the crew, allows better payload survivability and reduces the structural loadings along the Launcher.

The calculation of the most adequate trajectory will increase the launchers efficiency. By minimizing drag and gravity losses, a trade-off analysis needs to be performed [12, 21]. For the atmospheric flight, several works consider the use of gravity turn (GT). [21, 22, 23]. For the exo-atmospheric flight there are several methods for trajectory optimization used in works of the rocket design [24, 25, 22, 26].

It is often distinguished between two methods of numerical approaches in trajectory optimization, they are direct and indirect methods. In a first overview the direct methods consist in discretizing the state and the control and thus reduce the problem to a nonlinear optimization with constrains, and indirect methods consist of solving numerically boundary value problem derived form the application of the Pontryagin Maximum Principle and lead to the shooting methods. The paper of Betts gives a overview of the most common and popular numerical methods for trajectory optimization problems. However, it is difficult to reach with direct methods the precision provided by indirect methods [27]. The main advantages of using indirect methods are their high solution accuracy and the guarantee of satisfying the optimal conditions of the solution [28, 29].

Increasing the number of stages allows saving mass and adapting thrust and engines to the altitude where they will operate, but on the other hand, the design needs the minimum number of staging events, to maximize the overall system reliability [10]. In order to increase the reliability, and decrease the cost of transporting a payload into space, an extra effort is required during the initial design of the rocket and its trajectory, allowing saving money and time. Higher reliability does not directly result from reuse, since the necessary return capability, makes the launch vehicle more complex [30]. However, a noticeable cost reduction can only be achieved with high reuse rates, which depend on very high reliability systems. Due to the additional effort required to get the vehicle and/or stages back to Earth, reuse will be limited to launches into LEO (300-600 kilometres level and 100 degrees orbit inclination), at least regarding a near future. Ongoing missions (Geostationary Transfer Orbit (GTO)/ Geosynchronous Earth Orbit (GEO), Moon, interplanetary) will therefore, continue to require expendable upper stages. Reusability is considered to provide the major potential for future advancement of space transportation systems as it saves production costs, however, the complexity of the vehicle and the mission, increase along with the necessary return capability [2]. Typical objectives for reusable space launch systems are:

1. Cost reduction
2. Mission abort without loss of the launch vehicle
3. Return of payloads to the ground
4. Higher reliability

In analogy to aircraft, a fully reusable single-stage space transportation system, which delivers its

payload together with an expendable upper stage into LEO, is regarded as a goal. Various and sometimes very extensive US and European technology development and demonstration programs have shown, however, that substantial technological progress is necessary before the target of a fully reusable single-stage vehicle can be realized, particularly concerning: lightweight structures (tanks and high temperature thermal protection system), propulsion system performance (rocket and air-breathing propulsion). In the foreseeable future, only multistage and partly reusable space transportation systems are feasible [2, 31, 32, 33].

For future developments, a multitude of options are possible which lead to a variety of potential solutions. However, options that substantially affect the most important parameters, affecting the design, are limited: partial or full reusability (for a majority of missions expendable upper stages are necessary), number of stages of launch and landing method (horizontal, vertical, with/without propulsion, winged), propulsion (rocket, air-breathing propulsion, combinations) [24]. Based on experiences done with existing launch systems, extensive studies and technology activities, the following trends and limitations, for future developments, can be foreseen: single-stage vehicles need new technologies, reuse of boost stages leads to limited cost savings which do not justify the development and operating expenditure, air-breathing propulsion is very complex and its integration into the overall design is demanding and horizontal unpowered landing with wings is the feasible solution for the return of large rocket stages [34].

1.4 Work overview

Initially, rocket dynamics is presented, comprehending multistage rockets and learning the concepts of different ratios, like structural, mass and payload. Not only simple staging is considered, parallel staging is also taken into account and the propulsion technologies considered are solid, liquid and hybrid fuel, contemplating their advantages and disadvantages.

In the field of rocket trajectories it is important to solve the problem considering the vertical ascent phase and the gravity turn, because inside the atmosphere the ascent must be performed at zero lift because even a slight build-up of normal forces can destroy the rocket. For the last part of trajectory where the atmospheric forces are neglected an optimization method is used, a Two Point Boundary Value Problem (TPBVP).

The creation of a database, that gathers information about current and past launchers, allows achieving realistic results, and functions as a heuristic, regarding the field of design. To accomplish this, a tool is developed, in MATLAB, used, in a first stage, to design a rocket i.e. defining all the masses and dimensions, taking into account specific constrains. After, it is used to optimize the last part of the trajectory that fits such design, considering the Runge-Kutta integration during the ascent phase and gravity turn and the free-flight phase, where was used a TPBVP using shooting as optimization method. The ΔV losses are the key parameter for the convergence and achieve the final configuration. Two comparisons with real cases will be made to validate the mass model and the trajectory, and then a set of simulations, where the configuration and some parameters will be varied in order to optimize an existing Launcher.

Chapter 2

Rockets

In order to launch the satellites in orbit it's necessary to escape from the Earth's atmosphere and gravity. To accomplish that, a large amount of ΔV is necessary and with the current technology only rockets are able to achieve that. Currently, a SSTO is still impossible and only multistage configurations can achieve space, that allow to optimize the structure and propulsion of each stage for different conditions. Often, more than 90% of the rocket is propellant, meaning that rockets need a strong structure for accommodate all the propellants and its powerful engines to burn them. Their structure is long and thin allowing the reduction of drag during the trajectory. However this will bring structural problems when normal loads are applied in the structure.

2.1 Introduction to Rockets

The Tsiolkovsky's equation

$$V = V_e ln\left(\frac{m_0}{m}\right), \tag{2.1}$$

where V_e is exhaust velocity, m_0 the initial mass and m the mass of the rocket at each time. It allows the determination of the velocity increase of a rocket propelled vehicle, regarding the propellant consumption and the effective velocity of the exhaust gases. It is only valid for a constant exhaust velocity and in absence of external forces, such as atmospheric drag and gravity.

2.2 Delta-V calculations

The ΔV budget of a mission is represented as

$$\Delta V_{Design} = \Delta V_{orbit} + \Delta V_{gravity} + \Delta V_{drag}, \tag{2.2}$$

where ΔV_{orbit} is the injection velocity required for the desired orbit, $\Delta V_{gravity}$ and ΔV_{drag} are respectively the total gravity and drag losses. This equation allows us to make an estimate on the required ΔV consumption and thus the required fuel needed to reach the trajectory and lower earth orbit.The Drag

and Gravity Losses are the most significant losses in ascent trajectory. Other losses due to the manoeuvring and static pressure difference at the nozzle exit during flights are considerably smaller compared to gravity and drag losses. This ΔV budget must be larger or in exceptional cases equal to ΔV of the mission, otherwise the payload/spacecraft wouldn't be successful reaching the desired orbit.

The speed of a satellite in a circular orbit is defined by

$$V_{orbit} = \sqrt{\frac{\mu}{R}}, \tag{2.3}$$

where R is the radius of the orbit and μ the gravitational parameter of the planet.

The gravity loss is by definition

$$\Delta V_{gravity} = \int g \sin \gamma dt, \tag{2.4}$$

where g is the gravitational acceleration γ and the flight path angle. One way of reducing the gravity loss is to keep the flight path angle equal to zero. This scenario is impossible, since the launcher needs to achieve the desired orbit, but it is possible to strive for small flight path angle, as early as possible, to still achieve the mission altitude required.

The drag forces that take part on the launch vehicle are a function of the shape and size of the vehicle, his speed and angle of attack.

$$\Delta V_{drag} = \int \frac{D}{m} dt, \tag{2.5}$$

where D is the drag force and m the mass of rocket at each time. To optimize this ΔV the ascent movement must be slow, and as vertical as possible, and the mass must be high until the launcher rises in atmosphere, where the density will decrease. Once the rocket leaves the atmosphere the $Drag$ term goes to zero and thus no more drag is accumulated.

2.3 Configuration

2.3.1 Multi Stage

The single stage to orbit (SSTO) provides simplicity of design. However, the large inert mass that is associated with a SSTO rocket would be far more expensive than a multistage system, and an Earth-launched SSTO launch vehicles has never been constructed.

What characterizes it as "multi-stage" is that it successively jettisons one or more stages, as they become empty to save on the mass of the structure to reduce cost. The principal challenge of a rocket engineer is to achieve the lowest values of unnecessary mass possible in the vehicle. It is effectively by stacking on top one or more rockets (stages), or by attaching them next to each other ("parallel staging"), that will result in the reduction of the total amount of mass, which needs to be accelerated to the final speed/altitude.

In the figure 2.1 a multistage configuration of a rocket is presented.

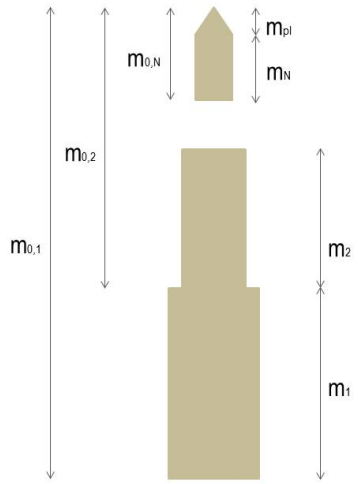

Figure 2.1: Multistage rocket configuration

Here m_N is considered a part of the rocket where the engine and tanks are and that is discarded after its extinction and m_{0N} is a rocket section. The payload of a particular rocket section is defined as being the mass of all rocket sections located above it. The payload of a specific stage is the mass of everything above that stage.

$$\lambda_N = \frac{m_{0N+1}}{m_{0N}}, \tag{2.6}$$

where m_{0N} is the total mass and m_{0N+1} is the mass of everything above that stage.

Total Payload Ratio is equal to the product of all payload ratios of all rocket sections and is equal to

$$\lambda_{tot} = \prod_{i=1}^{N} \lambda_i. \tag{2.7}$$

The Structural Ratio measures how much of the launch vehicle is structure, depends exclusively of the stage. Its value is dependent of technology and normally ranges between 0.08 and 0.2 [2].

$$\varepsilon_N = \frac{m_{sN}}{m_{sN} + m_{pN}}, \tag{2.8}$$

where m_{sN} and m_{pN} are respectively the structural and propellant mass of the N stage.

The Propellant Mass Ratio measures how much of the vehicle is propellant.

$$\varphi_N = \frac{m_{pN}}{m_{0N}} = (1 - \varepsilon_N)(1 - \lambda_N), \tag{2.9}$$

where m_{pN} and m_{0N} are respectively the propellant mass and the total mass of the N stage.

The Mass ratio is a measure of the efficiency of a rocket. For any given efficiency a higher mass ratio typically permits the vehicle to achieve higher ΔV.

$$\Lambda_N = \frac{m_{0N}}{m_{0N} - m_{pN}} = \frac{1}{1 - \varphi_N}, \tag{2.10}$$

where the m_{pN} and m_{0N} are respectively the propellant mass and the total mass of the N stage and φ is the propellant mass ratio.

The final burnout velocity is the sum of the burnout velocities of the individual stages, neglecting the gravity and atmosphere.

$$V_* = \prod_{i=1}^{N} V_{eN} \ln(\varepsilon_N + (1 - \varepsilon_N)\lambda_N) \tag{2.11}$$

The equations that described multistage rockets are almost equal as the single stage the term N doesn't exist [10].

2.3.2 Boosters

For larger payloads boosters stages are added to improve its performance, parallel staging in which two stages are burning at the same time. These boosters are attached to the first stage of the launch vehicle and their burn time is usually shorter than that of the first stage. Once they have burnt out they are instantly ejected.

In this particular case, a "zeroth" stage is defined as the combined booster rocket and first stage while they burn together, and the fist stage as the remaining part of first stage after the boosters have been discarded.

For "zeroth" the structural and payload ratios are [10]:

$$\varepsilon_0 = \frac{m_{s0} + m_{s1}}{m_{s0} + m_{s1} + m_{p0} + m_{p1}}, \tag{2.12}$$

$$\lambda_0 = \frac{m_{01} - m_{ip1}}{m_{00}}, \tag{2.13}$$

where m_{s0}, m_{p0} are respectively the structural, propellant ratio of the "zeroth" stage and m_{ip1} is the remaining propellant of the first stage when the "zeroth" stage burnout.

The equations for the remaining of first stage are [10]:

$$\varepsilon_1 = \frac{m_{s1}}{m_{s1} + (m_{p1} - m_{ip1})}, \tag{2.14}$$

$$\lambda_1 = \frac{m_{02}}{m_{02} + m_{s1} + (m_{p1} - m_{ip1})}, \tag{2.15}$$

where m_{02} is the total mass of second stage and everything above.

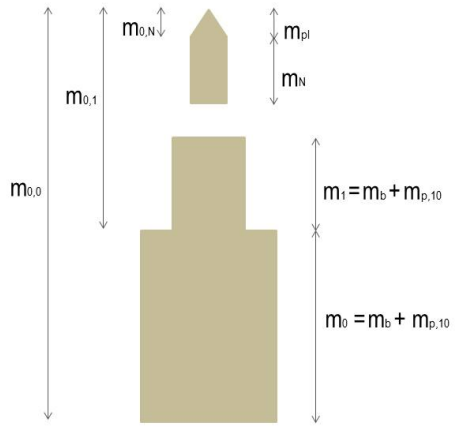

Figure 2.2: Parallel staging configuration

2.4 Structure

Every kilogram that is transported to space requires fuel, regardless whether that kilogram is cargo, crew, fuel, or part of the payload itself. The more the vehicle and the fuel weigh, fewer passengers and smaller the payload the vehicle can carry.

A launch vehicle system can be divided into 3 main categories: Lower stages, Upper stages and Fairing.

2.4.1 Lower Stages

Two basic functions take place in the lower stages. These are designed to both store the propellant required to fulfil the mission, as well as provide the structural stability required by the entire vehicle, they operate most of the time inside atmosphere. Usually, they are composed of a cylindrical section, which is mainly filled with propellant: in average, 90% of the total mass is propellant. The liquid propellants present in these vehicle stages, consist of fuel and oxidizer, which require the separation of each stage in different tanks. For solid propellant, the rocket stage itself is filled with propellant, which presents a typical grain section, with cylindrical or star form. The grain geometry defines the propellant mass flow rate, and burning time. For heavy launchers usually the first stage has boosters attached, they increase the payload mass that can be inserted in orbit.

In the figure 2.3(a). is possible to observe the characteristics described for a lower stage of the Vega rocket.

2.4.2 Upper Stages

The upper stage, usually the last stage, is active at higher altitudes, where the atmospheric effects are not so important as in the beginning of the flight and the vehicle's attitude can be improved because the

atmosphere forces can be neglected. This offers the advantage of a strict placement of the payload in the target orbit. However, it demands a dedicated and precise avionics system. Allied with the smaller dimension of the stage, this causes a higher structural ratio than the lower stages. Size then can became a problem, as the propellant mass is a function of the tank volume, whereas the structural mass is a function of the tank surface: with smaller tanks the ratio between surface and volume increases. Those stages are designed to operate at high altitudes, that allow to use low pressure in the combustion chamber and obtain a optimum nozzle expansion ratio without having a giant nozzle. In a typical launcher trajectory optimization, the guidance of the vehicle, in particular of the upper stage, is reduced to ensure that the attitude angle rates are lower than the upper limit, achievable by the control system of that stage.

In the figure 2.3(b) is possible to observe the characteristics previous described for an upper stage.

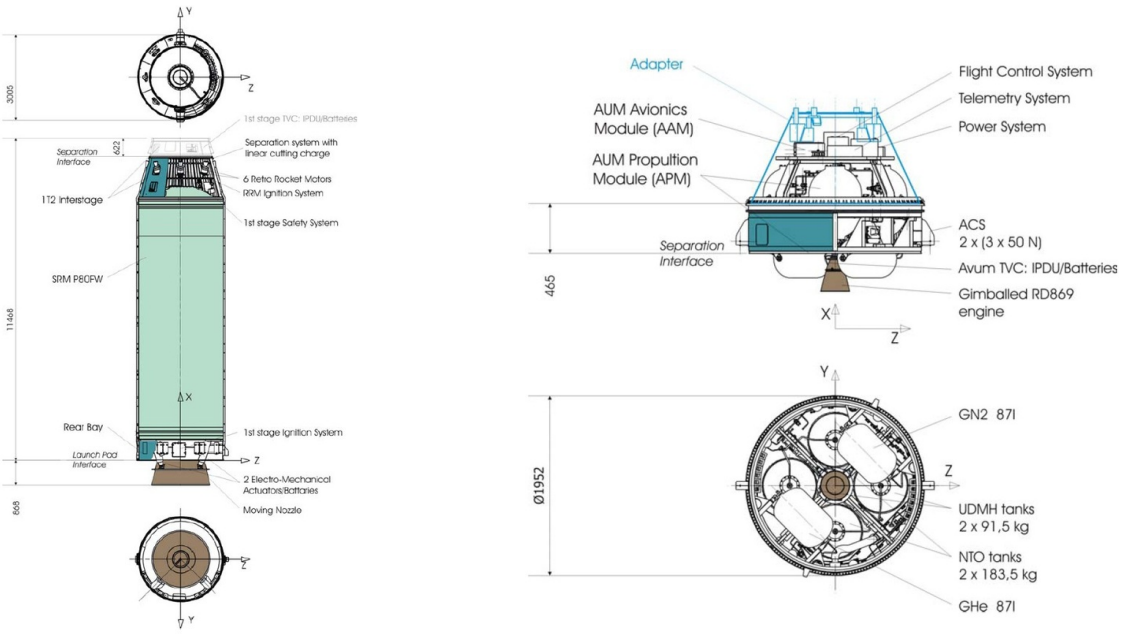

(a) Lower stage Vega

(b) Upper stage Vega

Figure 2.3: Lower and Upper Stage VEGA

[1]

2.4.3 Fairing

Placed at the tip of the rocket, a fairing has two main functions: diminish the atmospheric drag force and shield the payload from external loads, present in the early phases of the mission. Often it's jettisoned after the end of atmosphere. The shape of the fairing is therefore a compromise between a good aerodynamic effect and a high internal volume, required to accommodate the payload.

In the figure 2.4, is presented the Fairing used with the Vega launcher, where it's possible to observe the shape of Nose to reduce the drag forces and protect the payload.

[1] Arianespace.com

Figure 2.4: Fairing - Vega [2]

2.4.4 Other components

A launcher is composed of several additional components, most of these may however be considered part to the ones presented above: the mass of the interstage between stages 1 and 2 can be added to the structural mass of stage 1. This approximation will be accurate since the interstage is jettisoned together with the exhausted stage 1. Similarly the payload adapter mass should be incorporated in the upper stage structural mass. The payload, on the other hand, is treated differently in Volume but its mass is also integrated in the last stage.

In the figure 2.5 it's presented the interstage parts of the Vega rocket.

(a) Interstage 1-2 Vega

(b) Interstage 2-3 Vega

Figure 2.5: Interstage - Vega [3]

2.5 Propulsion

A launch vehicle needs a large velocity change, ΔV, to get from Earth's surface into orbit. Launch vehicles rely on their propulsion subsystems to produce this huge velocity change. After a spacecraft gets into space, its propulsion subsystem provides the necessary ΔV to take it to its final mission orbit.

The amount of thrust produced by the rocket depends on the mass flow rate through the engine and the exit exhaust velocity.

$$T = \dot{m}V_e - A_e(P_e - P_{amb}) \tag{2.16}$$

The main aspect regarding the nozzle is the altitude where it operates with maximum efficiency, which defines the nozzle area exit A_e. The ratio of areas of nozzle throat and exit is the nozzle area ratio. This means that for different stages or even during the same stages, the rocket will operate in different scenarios, and equilibrium is required, between small ratio areas for low altitude operations, and large ratio areas to allow the vacuuming along time. This is essential to achieve minimum mass and physical dimensions. In this study, the thrust was selected by the user and assumed constant during each stage, this result is a simplification, meaning the variation induced by the term $A_e(P_e - P_{amb})$ is neglected [21, 35, 36, 11].

"Specific impulse" is the amount of momentum gained per weight of fuel consumed, the unit is seconds, tells us the cost, in terms of the propellant mass, needed to produce a given thrust on a rocket. The g_0 is always the acceleration of gravity at the surface of the Earth. The great advantage is that the exhaust velocity Ve may be obtained in English or Metric units.

$$I_{sp} = \frac{V_e}{g_0} \tag{2.17}$$

Different technologies have their own strengths and weaknesses, and their performance differ considerably depending in which scenario are operating.

2.5.1 Solid Propellants

Solid propellant rockets have low specific impulse but relatively high storage density i.e. low volume, making them good solutions for volume-limited applications, including missiles as well as first-stage space boosters. Their I_{sp} normally ranges between 175 seconds and 285 seconds. Like other chemical rockets, they produce high thrust-to-weight ratios, and they are self-contained. Combustion of the propellant produces not only the energy but the working fluid for the rocket exhaust. There are no moving parts or pumping requirements. Once ignited, the rocket motor performs without complication. Nevertheless, the very simplicity of the solid-propellant motor connotes lack of control. There is little room for variation in the motor's performance once the propellant grain is ignited, and thrust vectoring is difficult. The solid rocket's thrust is proportional to the surface area of the burning propellant, which in turn is determined by the grain geometry. In all cases, the exterior shape of the grain is cylindrical, conical, or spherical; however, the interior geometry can be designed to produce a range of thrust profiles (or histories). The grain of an end burner is a solid cylinder, the burning surface has constant area as the propellant is consumed; the thrust is constant, relatively low, and of long duration. If a cylindrical core extends along the length of the motor, the initial surface is likely to be larger, hence, the thrust is larger and the burn time is shorter. Furthermore, the burning area increases as propellant is consumed, so

thrust increases up to the point at which all of the propellant has been used. In a heavy lift launch vehicle, solid propellant rockets are almost always built as a stand-alone system. In other words, they are built as boosters, which are strap on, high thrust, independent systems [20].

In the figure 2.6, we can observe a simple representation of Solid Rocket Propellant,where oxidizer and fuel are mixed together and cast into a solid mass called the grain and the hole down the middle called the perforation.

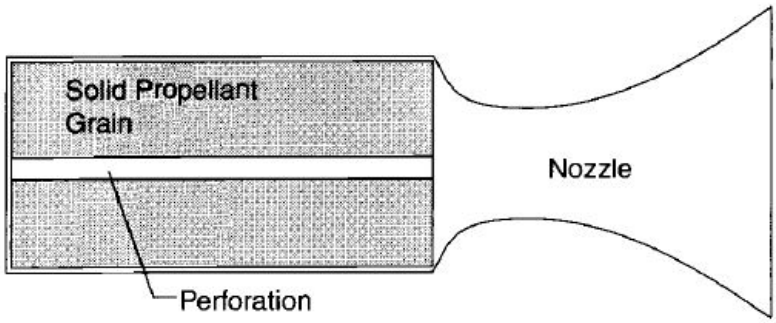

Figure 2.6: Solid Propellant Rocket Engine [37]

2.5.2 Liquid Propellants

Liquid propellant rockets require more complexity for basic operation, but their superior performance and precise controllability make them better suited for space applications. Their I_{sp} normally ranges between 200 seconds and 500 seconds. Mixing oxidizer and fuel is a critical issue; the penalty for poor combustion efficiency is severe, and the time during which the propellants must be combined is brief. Ignition should be self-sustaining once thrusting has begun. Cooling of the rocket's combustion chamber, throat, and nozzle is a considerable problem because high performance means high temperatures, the internal surfaces are exposed to high temperatures for long periods of time, and reliability and repeatability are important if the motor is to be restarted or reused. The highest performance propellants are gaseous at room temperature, and they must be cooled substantially for storage as liquids. This need for cryogenic storage and pumping produces practical difficulties. Propellants must be loaded into the vehicle shortly before launch, and there is an upper limit on the time that the propellants can be stored before they are used or they boil away. Storage in space can be prolonged by keeping propellant tanks shaded from sun light and by using tanks with high insulation, however, there are weight and volume limits on tank insulation. The pressure in the combustion chamber is high, and propellants must be raised to an even higher pressure to be injected into the motor. Pressurizing the fuel tanks and using high-pressure plumbing throughout is a practical solution only for very small installations, as the required weight is high. Pressurized, non-combusting or catalytic monopropellants have been used for the attitude control of small satellites. For large motors, a more practical approach is to use turbopumps to move the propellants, with pumps powered either by the rocket motor itself or by auxiliary power generators. Rocket nozzles for both solid- and liquid-propellant rockets must expand the flow efficiently. Early nozzles were simply

conical, as they were easy to build. However, most modern nozzles have a bell shape for more-efficient isentropic expansion. As noted earlier, a fixed expansion ratio can be matched to ambient pressure at just one altitude [20].

The mixture ratio of the propellant is normally specific to the engine and it represents the ratio between oxidizer and fuel. Usually it's represented with oxidizer mass as numerator and fuel mass as denominator.

$$MR = \frac{\dot{m}_{ox}}{\dot{m}_{fuel}} \tag{2.18}$$

The mass of oxidizer and fuel can be obtained by this two equations.

$$m_{ox} = \frac{(MR).m_{prop}}{(MR+1)} \tag{2.19}$$

$$m_{fuel} = \frac{m_{prop}}{(MR+1)} \tag{2.20}$$

In the figure 2.7, we can see a simple representation of Liquid Propellant Rocket,where the oxidizer and fuel are pumped into the combustion chamber.

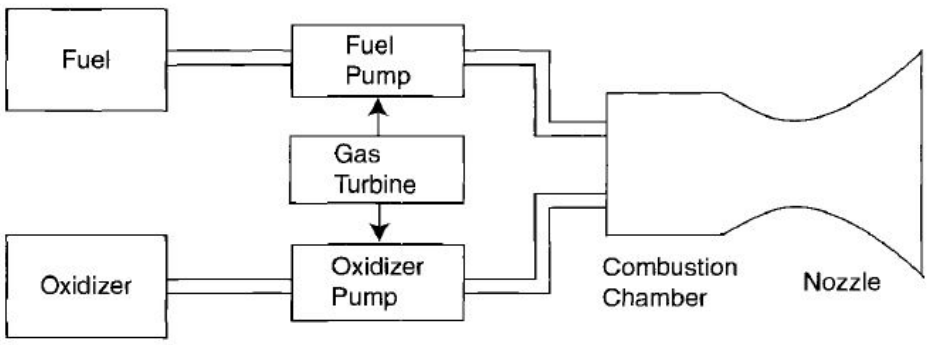

Figure 2.7: Liquid Propellant Rocket Engine [37]

2.5.3 Hybrid Propellants

Hybrid rockets store the fuel as a solid and inject the oxidizer as a liquid or gas. Combustion occurs along the grain surface, and it can be terminated by closing off the oxidizer flow. Their I_{sp} normally ranges between 260 and 400 sec. As might be expected, hybrid rockets have properties (good and bad) of both solid-propellant and liquid-propellant rockets. The principal advantages are that they allow energetic oxidizers (e.g., oxygen or hydrogen peroxide) to react with energetic fuels (e.g., hydrides of magnesium, aluminium, or beryllium), they can be throttled, and they have high volumetric specific impulse. Restarting and controlling thrust (magnitude and direction) are likely to be larger problems for hybrids than for liquid-propellant rockets, the specific impulse is not quite as high, and the cryogenic storage issue remains if liquid oxygen is used [20].

In the figure 2.8, we can see a simple representation of Hybrid Propellant Rocket,where the oxidizer

are pumped into the combustion chamber where is mixed with solid propellant.

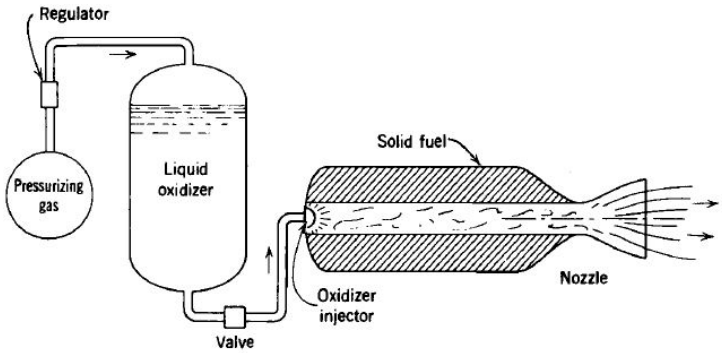

Figure 2.8: Hybrid Propellant Rocket Engine [37].

Chapter 3

Ascent Rocket Trajectories

The rocket flight can be divided in two main phases: the atmospheric flight and the exo-atmospheric flight. The frontier between them is not well defined, but can be linked to an altitude around 120 kilometres, where atmosphere forces can be neglected.

3.1 Trajectories

In this section a description of the different flight phases is made comprehending the different phases of the flight: the ascent phase, the gravity turn and the free-flight phase. Although the gravity turn guidance is not optimal, it's widely used in the trajectory of several works in rocket design. Only the last part in the free-flight phase was optimized where was used a Two Point Boundary Value Problem (TPBVP).

Then the section provides an overview of all the different models that are used to simulate the conditions that occur during the launch. Beginning with the drag model and then an overview of the environment which consists of an atmospheric model and the gravitational model.

3.1.1 Ascent Phase

A typical launcher starts its mission locked to the Launchpad. The engines are not yet ignited, or the thrust provided is still lower than the vehicle weight. For solid propulsion, the time between ignition and lift off is extremely short (less than 1 s). In the case of liquid propulsion, this time may be longer, allowing the verification of the correct engine operations, before releasing the vehicle.

The first phase is a vertical lift off, required to gain velocity before the gravity turn phase and avoid any contact with the launchpad tower. The duration of the ascent phase varies from vehicle to vehicle and the current tendencies is to decrease it, because of the developments made in technology. The necessary initial conditions include the flight path angle equal to 90 and velocity zero.

In the figure 3.1 is represented the launch sequence between lift-off and the final orbit, and the division of altitude in two parts, one where the atmosphere can't be neglected and other where the atmosphere is neglected.

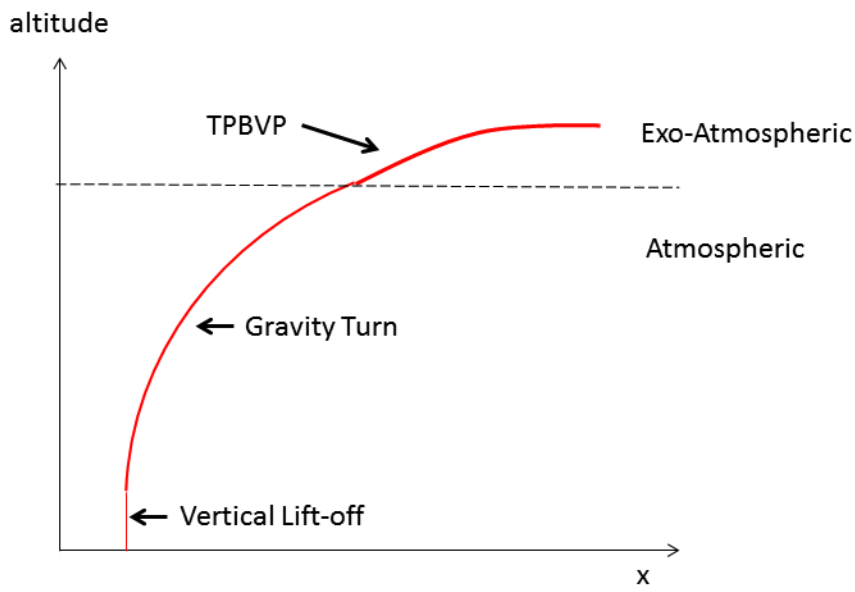

Figure 3.1: Launch Sequence.

3.1.2 Gravity Turn

The gravity turn phase, also named ”zero lift trajectory” is defined as a non-guided trajectory.

Primarily, the launch vehicle crosses the atmosphere, influenced by the drag and gravity forces. The angle of attack must be zero, because even a small angle of attack can lead to structural failure of the vehicle due to the large transversal forces that vehicle isn't prepared to stand. During the gravity turn trajectory, the vehicle slowly rotates its flight orientation, it goes from vertical to horizontal position, tangential to its orbit, due to the equilibrium of gravity and centripetal force. It also reduces the transverse aerodynamic stress on it, because it maintains the angle of attack zero.

Most launch vehicles have requirements of strength, regarding axial direction, that are fulfilled by compromising the structural strength in the transverse direction. As a result, they cannot fly at any significant angle of attack in the atmosphere, without risks of catastrophic failure of the whole structure. As a result, first stages of launch vehicles typically fly trajectories close to gravity turns (to minimize transverse loads). Contrarily, upper stages fly mostly outside of the atmosphere and therefore a better trajectory than the gravity turn can be used.

While the vehicle is given a small vertical nudge to begin the process, a small amount of lift is created, so the process should begin shortly after launch, when the vehicle's speed is still low. This process cannot be done in the initial launch position, because the vehicle does not have enough momentum and would fall over.

The equations of motion during the Gravity Turn are [10]:

$$\dot{X} = V cos\gamma, \tag{3.1}$$

$$\dot{H} = V sin\gamma, \tag{3.2}$$

$$m\dot{V} = T - D - (mg - \frac{mV^2}{Re + H})sin(\gamma), \tag{3.3}$$

$$\dot{\gamma} = -\frac{1}{V}(g - \frac{V^2}{Re + H})cos(\gamma), \tag{3.4}$$

where the X and H are respectively the downrange distance and altitude of the rocket, the V and γ are respectively the velocity and flight path angle of the rocket, the T and D are respectively the thrust and drag, the Re and m are respectively the radius of the Earth and the mass of rocket at each moment and g the local gravity.

The trajectory data includes altitude, flight path angle variation, thrust, drag and total system mass. In order to integrate the equations of movement a MATLAB standard solver for ordinary differential equations, commonly named ODEs, was used the function ode45. This function implements a Runge-Kutta method with a variable time step.

3.1.3 Free-flight phase

As the vehicle emerges from the atmosphere a better trajectory than the gravity turn can be used. It has a (present) position and velocity, and it is desired to achieve a different position and velocity at thrust termination. The only two forces that can cause the vehicle to accomplish the desired position and velocity changes are thrust and gravity.

Continuous problems of trajectory optimization are traditionally solved by direct or indirect methods [27]. We want to minimize the final time i.e. the duration of this phase, less time means less propellant because we assumed a constant thrust, this is therefore equivalent to minimize the GLOW. In boundary value problems, finding a good initial guess is a major difficulty. There is no formula, the engineer or the user must have some insight into the problem through numerical experimentation.

The TPBVP, only starts after the Knudsen number condition, that tell us that we are in exo-atmospheric conditions. Here the drag forces are neglected. This problem was solved numerically by a shooting method, based on the application of the Pontryagin Maximum Principle. The shooting method is known to be hard to initialize, and the convergence is difficult to obtain because of discontinuities of the optimal control [38].

For minimum time problems [28], the cost function can be written as

$$J = t_f, \tag{3.5}$$

subject to 4 state equations

$$\dot{x} = V_x \tag{3.6}$$

$$\dot{y} = V_y \tag{3.7}$$

$$\dot{V_x} = \frac{T}{m_0 - \dot{m}t} cos(\theta) \tag{3.8}$$

$$\dot{V_y} = \frac{T}{m_0 - \dot{m}t} sin(\theta) - g \tag{3.9}$$

the initial conditions of TPBVP are the final conditions of gravity turn.

$$t_0 = t \tag{3.10}$$

$$x_0 = x \tag{3.11}$$

$$y_0 = y \tag{3.12}$$

$$V_{x0} = V_x \tag{3.13}$$

$$V_{y0} = V_y \tag{3.14}$$

the final conditions, for the particular case of circular orbit are

$$y_f = R_e + h \tag{3.15}$$

$$V_{xf} = Vc \tag{3.16}$$

$$V_{yf} = 0 \tag{3.17}$$

condensed as

$$\Psi = \begin{bmatrix} \Psi 1 \\ \Psi 2 \\ \Psi 3 \end{bmatrix} = \begin{bmatrix} y_f - (R_e + h) \\ V_{xf} - V_c \\ V_{yf} \end{bmatrix} = 0 \tag{3.18}$$

We know that t_f and x_f are free variables. The Hamiltonian is

$$H = \lambda_1 \dot{X} + \lambda_2 \dot{Y} + \lambda_3 \dot{V_x} + \lambda_4 \dot{V_y} \tag{3.19}$$

The Euler-Lagrange Equations $\dot{\lambda} = -H_x, H_u = 0$, so the costate equations are.

$$\dot{\lambda}_1 = -\frac{dH}{dx} = 0 \tag{3.20}$$

$$\dot{\lambda}_2 = -\frac{dH}{dy} = 0 \tag{3.21}$$

Thus

$$\lambda_1 = c_1 \tag{3.22}$$

$$\lambda_2 = c_2 \tag{3.23}$$

$$\dot{\lambda}_3 = -\frac{dH}{dv_x} = -\lambda_1 \tag{3.24}$$

$$\dot{\lambda}_4 = -\frac{dH}{dv_y} = -\lambda_2 \tag{3.25}$$

Since the λ_1 and λ_2, are constant

$$\lambda_3 = -c_1 t - c_3 \tag{3.26}$$

$$\lambda_4 = -c_2 t + c_4 \tag{3.27}$$

The control equation is found from

$$\frac{dH}{d\theta} = -\lambda_3 \frac{T}{m} sin(\theta + \lambda_4 \frac{T}{m} cos(\theta) = 0 \tag{3.28}$$

Thus, we have, a bi-linear tangent law.

$$tan(\theta) = \frac{\lambda_4}{\lambda_3} = \frac{-c_2 t + c_4}{-c_1 t + c_3} \tag{3.29}$$

and then

$$cos(\theta) = (\frac{\pm\lambda_3}{\sqrt{\lambda_3^2 + \lambda_4^2}}) \tag{3.30}$$

$$sin(\theta) = (\frac{\pm\lambda_4}{\sqrt{\lambda_3^2 + \lambda_4^2}}) \tag{3.31}$$

Applying transversality condition and the Minimum Principle, which states that the Hamiltonian must be minimized [28]. We have a $\lambda_1 = c_1$ and $\lambda_{1f} = c_0$, so $c_1 = 0$. Therefore we obtain the linear tangent steering law.

$$tan(\theta) = \frac{c_2 t}{-c_3} + \frac{-c_4}{-c_3} = at + b, \tag{3.32}$$

this law is used in guidance systems, with updates for a and b at each second.

At this point, we have a well defined TPBVP, with four state equations, and four costate equations.

$$\dot{x} = V_x \tag{3.33}$$

$$\dot{y} = V_y \tag{3.34}$$

$$\dot{V_x} = \frac{F}{m_0 - \dot{m}t}(\frac{-\lambda_3}{\sqrt{\lambda_3^2 + \lambda_4^2}}) \tag{3.35}$$

$$\dot{V_y} = \frac{F}{m_0 - \dot{m}t}(\frac{-\lambda_4}{\sqrt{\lambda_3^2 + \lambda_4^2}}) - g \tag{3.36}$$

$$\dot{\lambda}_1 = 0 \tag{3.37}$$

$$\dot{\lambda}_2 = 0 \tag{3.38}$$

$$\dot{\lambda}_3 = -\lambda_1 \tag{3.39}$$

$$\dot{\lambda}_4 = -\lambda_2 \tag{3.40}$$

Thus there are eight differential equations.

$$\dot{x} = f(t, x, \lambda) \tag{3.41}$$

$$\dot{\lambda} = g(t, x, \lambda) \tag{3.42}$$

Now there are five initial conditions and five final conditions.

The steps that shooting method uses are the following:

1. Guess $\lambda_{10}, \lambda_{20}, \lambda_{30}, \lambda_{40}$ and t_f
2. Integrate the $\dot{x}$ and $\dot{\lambda}$ forward to $t = t_f$
3. Compute the final conditions:

$$\Psi 1 = y_f - h_{circ} + R_{Earth} \tag{3.43}$$

$$\Psi 2 = V_{xf} - V_{circ} \tag{3.44}$$

$$\Psi 3 = V_{yf} \tag{3.45}$$

$$\Psi 4 = \lambda_{1f} \tag{3.46}$$

$$\Psi 5 = H_f + 1 \tag{3.47}$$

   where λ and t_f are changed iteratively

4. Until the convergence on $\Psi i(\lambda_{0,tf}) = 0$ for $i = 1, .., 5$

In the figure 3.2, it's possible to observe, the initial conditions, and a few iterations of Shooting Method until the convergence has achieved.

To solve this last part of the trajectory a Matlab function has been used. The bvp4c solves boundary value problems for ordinary differential equations. For many optimal control problems, as in our case, is the best option. However, we must pay attention to the limitations of bvp4c, more specifically a good initial guess is important to get an accurate solution, if a solution exists. By applying the minimum principle, we can convert the problem into a BVP and solve it with indirect methods. Nevertheless, for problems with constraints, does not necessarily hold although the Hamiltonian still achieves the minimum within the admissible control set [28].

3.1.4 Coast Phases

The coast phases are performed between the jettison of a stage and the ignition of the next one. So the propagation of the trajectory is only influenced by the gravitational force, in real cases aerodynamic

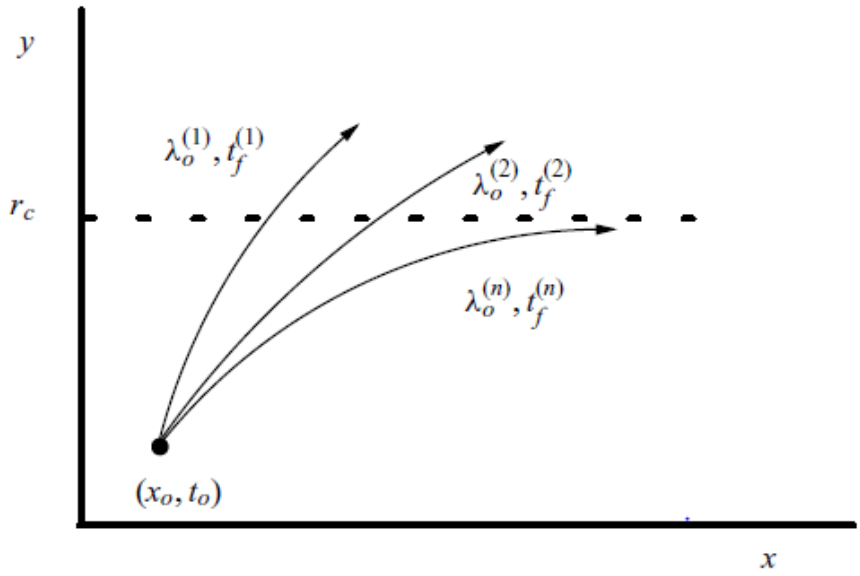

Figure 3.2: Shooting Method for the free-flight phase

forces need to be considered, but in this case as we know there is no angle of attack during atmospheric flight so they can be disregarded. The coast phases are often used for injection into GTO and for interplanetary trajectories, where the constant thrust can't be applied.

3.1.5 Drag Model

The drag coefficient is a function of the atmospheric conditions (local flow Mach number) and the geometry of the rocket. Obtaining information of aerodynamic data launchers is almost impossible, because this data is kept secret. To be more precise a Computational Fluid Dynamics (CFD) analysis is needed to get results closer to reality. An approach for analytical formulas for each Nose Cone was tried, but lack of available information didn't allow to go further in that analysis [39]. An assumption was made, the drag force is independent of the length of the vehicle (assuming skin friction drag to be negligible).

$$D = \frac{1}{2}\rho C_D S_{ref} V^2, \tag{3.48}$$

where ρ is the density of the atmosphere, the C_d is the drag coefficient, S_{ref} is the cross-sectional area of the body and V is the velocity of the vehicle.

A simple model for the C_d was adopted [40]. An interpolation of the values for the first stage from table 4.16 in page 269 was made. The C_d only varies with the Mach Number. The resulting equation is

$$C_d = -3E^{-6}M^6 + 0.0002M^5 - 0.0046M^4 + 0.053M^3 - 0.2806M^2 + 0.6211M + 0.0568 \tag{3.49}$$

This equation have a regression of 90% with a polynomial fit of 6th order.

The program shows the dynamic pressure during atmospheric phase

$$q = \frac{1}{2}\rho V^2, \tag{3.50}$$

where ρ is the air density and V the velocity of the rocket.

The dynamic pressure has two important properties. The quadratic dependence on velocity means that the lift and drag increase very rapidly as the rocket accelerates. The effect of drag on first-stage acceleration is significant, the acceleration of the vehicle is often almost constant even though the mass is reducing. The dynamic pressure also depends on the atmospheric density, which decreases rapidly as the rocket gains altitude. Thus, with velocity increasing, and density decreasing, with time after launch, every launcher passes through a condition known as maximum dynamic pressure that happens around an altitude of about 10 kilometres. This is the time when the atmospheric forces are at their maximum, and when the risk to the structural integrity of the rocket is greatest. To reduce the risk, if the vehicle's structure isn't designed to support the loads it experiences, the engines are throttled down in order to reduce the forces acting on the vehicle. The figure 3.3 shows how the Dynamic pressure varies with altitude.

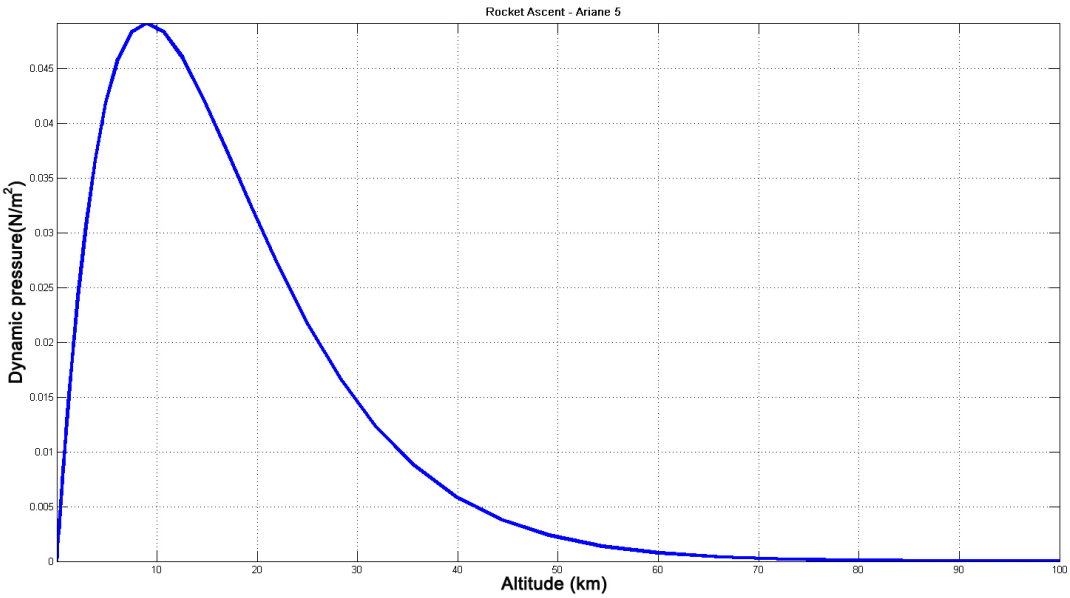

Figure 3.3: Dynamic Pressure

3.1.6 Atmospheric Model

The earth atmosphere is a thin layer around the planet and during the flight to orbit the performance of the launch vehicle will be influenced by its environment.

Therefore, it is important to understand and model the atmosphere's properties (temperature, pressure and density) with accurate approximations. Many atmospheric models have already been developed to answer the needs of the design of launch vehicles and the analysis of their trajectory.

In 1962 and 1976, two U.S conventions of Standard Atmosphere were developed, the first regarding velocities for altitudes higher than 86 kilometres, and the second one regarding velocities for altitudes lower than 86 kilometres [41].

In this work, the U.S. Standard Atmosphere Convention of 1976 was used as a reference, for altitudes lower than 86 kilometres, and the 1962 U.S. Standard Atmosphere was followed for altitudes above 86 kilometres, it models atmosphere up to 2000 kilometres. The last layer ranges between 700 and 2000 kilometres [35].

The Knudsen number will define the boundary between the atmospheric and exo-Atmospheric flight, i.e. it will define the end of gravity turn and the beginning of the third part of flight. The Knudsen number is dimensionless defined as

$$Kn = \frac{\lambda_{kn}}{L} \tag{3.51}$$

In equation 3.51, λ_{kn} is the mean free path of free-stream molecules and L is a length characteristic, the value assumed was the cone radius that it's the same of last stage radius. The different flow regimes are classified as shown below:

$$ContinuumFlow \qquad Kn < 0.01 \tag{3.52}$$

$$TransitionFlow \qquad 0.01 < Kn < 10 \tag{3.53}$$

$$Free - MolecularFlow \qquad Kn > 10 \tag{3.54}$$

The next figure 3.4 represents the variation of Density along the first 120 kilometres of the Atmosphere, where the effects of Drag can't be neglected.

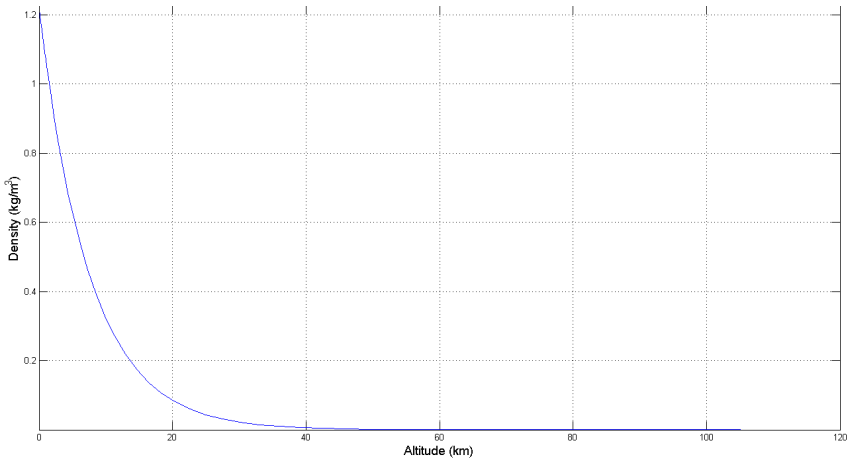

Figure 3.4: Atmospheric Density

3.1.7 Gravitational Model

The external force caused by gravity is the main force that acts on the launch vehicle. Gravity is the natural phenomenon by which physical bodies are attracted to each other with a force proportional to

their masses. This work assumed a flat and non-rotating Earth so that g_0 is constant and terms involving its angular velocity are ignored [21].

The local gravity is calculated with the following equation

$$g = \frac{g_0}{1 + \frac{h}{R_e}}, \tag{3.55}$$

where h is the current altitude, $R_e = 6378$ kilometres the radius of Earth and $g_0 = 9.81(m/s)$ surface gravity.

Chapter 4

Rocket Knowledge Database

For a better understanding of the differences between launchers, and to compare converging parameters between them, a database of well-known launchers was developed. It gathers information about their different masses, dimensions and propulsion, to understand if the concept of new designed rockets is ”real”, and if their values can be compared with similar launchers. The database can also be used as a starting point or to help define bounds of parameters.

4.1 DB construction development

Although there is information available about more than a hundred launch rockets, only four to five were considered, for each class. The database was developed and divided by ”how much payload they can deliver in specific orbit?”. Regarding this criteria three different classes of launchers were defined.

4.1.1 Small

Small launchers are mainly used for transferring payloads into Low Earth Orbit (LEO), they can deliver up to 2 tons at LEO [2]. Information about four launchers of this class was gathered, they are Rockot [42], Pegasus-XL [43], Falcon 1 [44] and Vega [4]. None of them have boosters in their configuration.

4.1.2 Medium

Medium launchers serve to place satellites into all Earth orbits: LEO, including polar orbits, medium Earth orbits (MEOs), GTOs, GEO and Earth escape missions. They can deliver between 2 and 15 tons at LEO and 3 to 6 tons at GEO [2]. These kind of launchers feature the possibility of having boosters. Information about 5 launchers was gathered, they are Soyuz [45], CZ-4B, Zenit-SL [46], H-IIA and Delta IV-M [47].

4.1.3 Heavy

Heavy-lift launch vehicles (HLLVs) mainly launch communications satellites into GTOs and are used specifically for launching very heavy payloads. They can deliver more than 15 tons at LEO and 6 tons at GEO [2]. Except some launchers, they all have boosters. They have long burning times of first-stage, i.e. they spend more time leaving the Earth atmosphere, compared to Small and Medium launchers. Information about 4 launchers was gathered, they are Ariane 5 [48], Proton K-DM3 [5], Atlas V [49] and STS known as Space Shuttle [3].

4.2 Information gathered

For each stage of each launcher a lot of information was available in the Users Manual but only the principal characteristics that define a rocket were selected. In the table 4.1 are a list of the information gathered for the selected launchers.

Characteristics	Units
Class	Small/Medium/Heavy
Year	-
Engine	-
Length	m
Diameter	m
Length/Diameter	-
Take-off mass	kg
Propellant mass	kg
Structural mass	kg
Structural factor	kg
Propellants	-
Burning duration	s
Thrust (vac)	kN
Isp (vac)	s
T/W	-
Remarks	-

Table 4.1: Characteristics gathered for each Stage of each Launcher

Some information wasn't available for all launchers, for example the Nozzle Area Ratio is one characteristic that is very difficult to obtain, such as Aerodynamic Performance. The most important information gathered is about structural factor of each stage, that allows us to know how much mass of each stage is structure, and to give an appropriate range of values of Structural factor of each stage for Mass model developed in this work. The medium value obtained was used in mass model as first value for the iterations of Structural factor. The range of values is presented in the table 4.2.

	Min	Medium	Max	Class
1 Stage	0.057	0.073	0.085	Small
2 Stage	0.073	0.090	0.095	Small
3 Stage	0.095	0.152	0.21	Small
4 Stage	0.124	0.153	0.193	Small
Booster	0.087	0.101	0.115	Medium
1 Stage	0.049	0.086	0.119	Medium
2 Stage	0.095	0.117	0.153	Medium
3 Stage	0.065	0.131	0.171	Medium
Booster	0.080	0.117	0.149	Heavy
1 Stage	0.039	0.063	0.076	Heavy
2 Stage	0.069	0.131	0.239	Heavy
3 Stage	0.082	0.121	0.182	Heavy
4 Stage	0.134	0.172	0.195	Heavy

Table 4.2: Structural factor for each Stage

The same approach was used for thrust, regarding each stage of each category. The minimum, maximum and medium values of Thrust were gathered.The values are presented in the table 4.3. These values concern Thrust in vacuum, and will certainly be less if operating inside the atmosphere.

	Min	Medium	Max	Class
1 Stage (kN)	320	896.5	2092	Small
2 Stage (kN)	33.6	346.4	959	Small
3 Stage (kN)	19.62	94.74	230	Small
4 Stage (kN)	2.2	6.8	13.2	Small
Booster (kN)	608.1	709.5	810	Medium
1 Stage (kN)	780	3197.6	7850	Medium
2 Stage (kN)	110	424.78	833	Medium
3 Stage (kN)	19.6	67.86	100	Medium
Booster (kN)	1655	6601.6	11790	Heavy
1 Stage (kN)	1350	2324	4152	Heavy
2 Stage (kN)	62.8	755.5	2278	Heavy
3 Stage (kN)	582	1362	2472	Heavy
4 Stage (kN)	87	255	467	Heavy

Table 4.3: Thrust in Vacuum for each Stage

Another important information is the Length/Diameter ratio. This ratio gave us the idea of how the dimensions vary for different stages, for example the difference of increasing one meter of diameter in first stage or in the last stage are considerably different. The values are presented in the table 4.4.

	Small	Medium	Heavy
Booster	-	7.313	11.99
1 Stage	5.823	8.574	6.241
2 Stage	2.647	2.728	2.771
3 Stage	1.48	0.874	1.002
4 Stage	0.99	1.05	0.87

Table 4.4: Length/Diameter ratio

Also, the principal characteristics about payload fairing, which were also gathered for each launcher, are listed in the table 4.5.

Characteristics	Units
Volume	m^3
Mass	kg
Length	m
Diameter	m
Length/Diameter	-
Payload	kg

Table 4.5: Characteristics of Payload Fairings

With the information gathered about the Payload, an estimate of how much of GLOW is from Fairing. This information provides us a good estimate for the mass of the Fairing and its presented in the table 4.6.

	Small	Medium	Heavy
% $Mass_{fairing}/GLOW$	0.92	0.96	0.9

Table 4.6: Ratio between Mass Fairing and GLOW

The GLOW is already defined and the mass of Fairing is estimated by a heuristic relation. A relationship between the mass and the volume of the Fairing was developed, for each class of launchers. An exponential regression was used for the following equations:

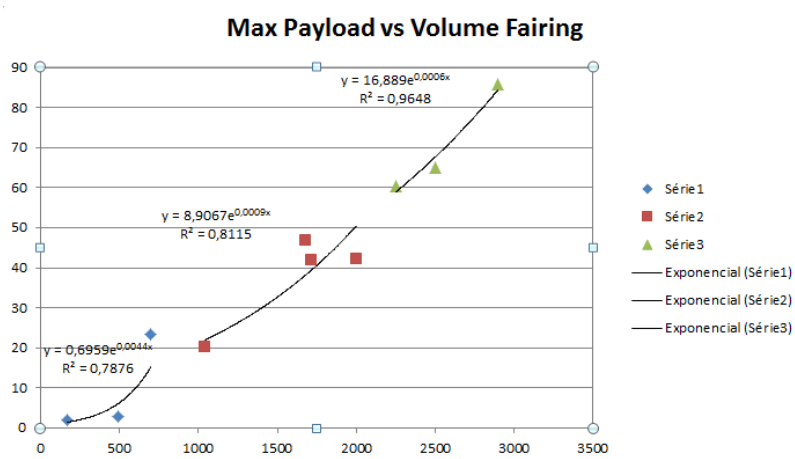

Figure 4.1: Max Payload vs Volume Fairing

For the class of Small Launchers, the Volume is defined by

$$V_{fairing} = 0.6959e^{0.0044M_{fairing}} \tag{4.1}$$

For the class of Medium Launchers, the Volume is defined by

$$V_{fairing} = 8.9067e^{0.0009M_{fairing}} \tag{4.2}$$

For the class of Heavy Launchers, the Volume is defined by

$$V_{fairing} = 16.889e^{0.0006M_{fairing}} \tag{4.3}$$

The Fairing is included in the last stage. So the diameter of the base of Nose Cone will be equal to the diameter of the last stage. Knowing the Volume, and the type of Nose Cone (more in Appendix A), there is enough information to design the Fairing from the initial design point of view. The length of the Nose Cone is added to the rest of the launcher to calculate the total dimensions of the Launcher.

The volume of an Elliptical cone is defined by

$$V_{EllipticalCone} = \frac{\pi d^2 h}{6}, \tag{4.4}$$

with this formula, knowing the Volume and the diameter (d), all the dimensions are obtained and the Nose Cone can be included in the calculations.

4.3 Propellant Selection

For the selection of propellant, various propellants were researched, for analysis and selection, as described in the previous sections. Limiting the number of propellants for the model analysis, based on Specific Impulse (I_{sp}), narrowed down the propellants. With this, a set of twelve propellants was provided, from different categories: liquid, hybrid, and solid. This list of propellants is used in the mass model simulations.

The Engine performance is generally specified in terms of I_{sp}. Naturally it is essential to select a propellant with the highest I_{sp} possible. However, other considerations regarding safety and storability must be taken in account. The table 4.7 shows a list of several propellants and their associated specific impulses.

Propellant	Specific Impulse (Isp)	Units	Type
LOX/H2	462	Seconds	Liquid
LOX/Hydrazine	363	Seconds	Liquid
LOX/RP1	347	Seconds	Hybrid
Nitrogen Tetroxide/RP1	328	Seconds	Liquid
Nitrogen Tetroxide/HTPB	297	Seconds	Hybrid
LOX/HTPB	317	Seconds	Hybrid
F2/H2	441	Seconds	Liquid
Nitrogen Tetroxide/MMH	318	Seconds	Liquid
Nitrogen Tetroxide/UDMH	313	Seconds	Liquid
Nitrogen Tetroxide/Hydrazine	309	Seconds	Liquid
HTPB/AP	260	Seconds	Solid
DB/AP-HMX	265	Seconds	Solid

Table 4.7: Propellant Specifications [1]

All specific impulses are at sea level conditions. Information about the Mixture Ratio, and density was gathered for each combination of propellant, and is available in the Appendix B. This will provide

more realistic results for the results of the mass model.

4.4 Mass Estimation Relationships

Mass estimation techniques regarding aerospace vehicles, have been developed to be used in conceptual design phase. These techniques are based on historical data, including existing or previously flown spacecraft and launch vehicles. With the improvement of technology, it's becoming more and more difficult to derive good mass estimations, during conceptual phases of design.

Historically, information has been gathered and a few models have been developed over the world. In Maryland University, Professor Akin developed a model of Mass Estimation Relationships (MERs) [50] [1]. The equations that derive from this model will provide a heuristic comparison between the values obtained for structural mass in the mass model designed for this work and those obtained from heuristics, searching for convergence.

The MER for Thrust Structure Mass is

$$M_{ThrustStructure}(kg) = 2.55 \cdot 10^{-4} T(N), \tag{4.5}$$

where T is the thrust of the engine.

The MER for the Casing of Solid Rocket Motor is

$$M_{MotorCasing}(kg) = 0.135 \cdot M_{prop}(kg), \tag{4.6}$$

where M_{prop} is the propellant mass.

The MER for Engine Mass is

$$M_{Engine}(kg) = 7.81 \cdot 10^{-4} T(N) + 3.37 \cdot 10^{-5} T(N) A_r^{0.5} + 59, \tag{4.7}$$

where A_r is the nozzle area ratio and T the thrust of the engine.

A generalisation was done, simplifying the equation shown below of the Mass of Oxidizer Tank, adapting it for liquid and hybrid rockets. For each situation, the LOX special case was considered.

$$M_{LOX_{Tank}}(kg) = 0.0107 \cdot M_{LOX}(kg), \tag{4.8}$$

where M_{LOX} is the mass of the oxidizer.

The same was done for the Mass of Fuel Tank, taking into account the LH2 special case for every situation.

$$M_{LH2_{Tank}}(kg) = 0.128 \cdot M_{LH2}(kg), \tag{4.9}$$

where M_{LH2} is the mass of the fuel.

[1] spacecraft.ssl.umd.edu/academics/academics.html

The MER for the Mass of Fuel Tank, special case RP-1.

$$M_{RP-1_{Tank}}(kg) = 0.0148 \cdot M_{RP1}(kg), \tag{4.10}$$

where M_{RP1} is the mass of the fuel for the special case $RP1$.

The MER for Mass of LOX insulation Tank is

$$M_{LOX_{InsulationTank}}(kg) = 1.123(kg/m^2) \cdot A_{surfaceofLOXtank}(m^2), \tag{4.11}$$

where $A_{surfaceofLOXtank}$ is the surface area of the oxidizer tank.

The MER for Mass of LH2 insulation Tank is

$$M_{LH2_{InsulationTank}}(kg) = 2.88(kg/m^2) \cdot A_{surfaceofLH2tank}(m^2), \tag{4.12}$$

where $A_{surfaceofLH2tank}$ is the surface area of the fuel tank.

In this two previous cases, a sphere was assumed

$$V_{LOX_{Tank}} = \frac{M_{LOX}}{\rho_{LOX}}, \tag{4.13}$$

the radius is

$$r_{LOX_{Tank}} = \frac{V_{LOX}}{4\pi/3}^{\frac{1}{3}}, \tag{4.14}$$

so, the Surface Area is

$$A_{LOX_{Tank}} = 4\pi r_{LOX_{Tank}}, \tag{4.15}$$

The same equations are applied to $LH2$ tank.

Mass of Fairing, is estimated from is Area, this MERs only applies in the Last Stage.

$$M_{fairing}(kg) = 4.95 \cdot (A_{fairing}(m^2))^{1.15}, \tag{4.16}$$

where $A_{fairing}$ is the fairing surface area.

Mass of Avionics, only depends of GLOW.

$$M_{avionics}(kg) = 10(M_0(kg))^{0.361}, \tag{4.17}$$

where M_0 is the total mass of each stage.

The Akin model doesn't consider interstage part as an important mass to be estimated, so there is no MER for this case. Others Mass Estimation Relationships Estimations have been developed such as Zanderberg, Apel, NASA and in MDO PhD Thesis [51, 52, 53, 16, 54]. Other heuristics are used in this work, such as preliminary estimation of Gravity and Drag Losses. Those heuristics are based in Wittmann book [2]. A good preliminary estimation of this parameters will allow the program to save time during its iterations. Those preliminary estimations depends on the altitude of the selected orbit.

$$\Delta V_{gravity} = 0.08 < V_{orbit} < 0.12 \tag{4.18}$$

$$\Delta V_{drag} = 0.008 < V_{orbit} < 0.012 \tag{4.19}$$

The initial values selected were $\Delta V_{gravity} = 0.12 \cdot V_{orbit}$ and $\Delta V_{drag} = 0.009 \cdot V_{orbit}$, because those were the values that most decreased the velocity of the simulations.

Other Heuristic, for the same variables, but depending on Initial T/W.

$$\Delta V_{gravity} = 81.006 \left(\frac{T}{W}\right)^2 - 667.62 \left(\frac{T}{W}\right) + 1505.4 \tag{4.20}$$

$$\Delta V_{drag} = -32.692 \left(\frac{T}{W}\right)^2 + 258.86 \left(\frac{T}{W}\right) - 226.57 \tag{4.21}$$

This different approach, shows us how the gravity and drag losses, depend on $\frac{T}{W}$. The faster the rocket flies in the dense atmosphere the drag losses will also increase. But on other hand for a lower value of $\frac{T}{W}$, the rocket will take more time to escape from the strong gravitational force from the Earth and more time to achieve the target orbit. This approach can't be used in our mass model because as its going to be explained in the next chapter the mass model receives as input a $\Delta V_{estimate}$ and only after the mass model was run, the initial value of $\frac{T}{W}$ is calculated [2].

[2] https://www.open-aerospace.org/rocket-sizing

Chapter 5

Rocket Design Tool

A tool was developed to help the preliminary design of a rocket. In this difficult task some design parameters were selected as input and others were calculated from the selected ones. The values and the variation of the input parameters were selected by the user.

The computer simulation program was designed to perform a rocket optimization. This means that it optimizes all the masses and the dimensions of the vehicle as well as the last part of the trajectory. To develop this work a Matlab code was developed, in order to design the rocket and simulate trajectories into orbit.

There is the possibility to optimize performance by minimizing the take-off mass of the launch system, for a given payload and target orbit. However, minimum take-off mass does not necessarily mean minimum costs, and minimum costs might be the costs for a single mission or those of the complete life cycle of the system, including development.

5.1 Program Overview

The program was divided in two main parts: first, the mass model and second, the trajectory. They were developed separately, but depending on each other for complete design of a launch vehicle.

The mass model together with the trajectory will get the minimum GLOW and maximum payload ratio for the purposed objectives (orbit altitude and payload mass), depending on user's choices (Number of Stages, Boosters, Propellant, Diameter, Thrust and Nozzle Area Ratio for each stage and ΔV Division) and the variation of these parameters. For each combination of parameters all the masses and dimensions are defined and then the trajectory will give the best trajectory that suits the configuration designed before. The program achieves the final configuration when the ΔV used in mass model matches the ΔV of the trajectory. For each combination of parameters a minimum GLOW is calculated. After all simulations done, the program selects the combination of parameters that achieve a minimum GLOW.

5.2 Parametrization

The key parameters, that most influence the program, are:

1. ΔV Losses, a good estimate, increases the efficiency of the code.
2. Structural Ratio, to achieve realistic results for the Dry Mass.
3. End of the atmosphere, defined by the Knudsen number will define where the Gravity Turn ends and the free-flight phase of the trajectory starts.

5.3 Algorithm

In this section is described how the tool achieves the best configuration for one combination of parameters and configuration. This algorithm is repeated for all the combination of parameters and configurations.

First, the user inputs his objectives: the orbit altitude and the payload mass. Then the user has to make basic decisions about the configuration: how many stages there will be (between two and four) and if boosters will be used in the first stage and how many there will be. It is assumed that the launch system starts from ground, with velocity equal to zero and launch from vertical.

The first ΔV evaluation assumes an estimate for gravity and drag losses as shown in the chapter 4 [2]. A good preliminary estimate of ΔV losses increase the velocity of program, i.e. the tool will need less iterations to find the best solution.

Before the user enters the mass model, had already selected the configuration and some parameters, listed in the table 5.1, and its variation for each stage:

Characteristics	Units
Number of Stages	-
Number of Boosters	-
Diameter Booster	m
Diameter	m
Nozzle Area Ratio	-
Propellant Selection	-
Thrust	kN
Thrust Booster	kN
ΔV division	-

Table 5.1: Configuration and parameters introduced in the tool.

The propulsion parameter selected was the thrust instead of burn time. Due to the creation of database, the user can have an insightful idea of the values of thrust, for each stage and different payload masses. The burn time is obtained after defining the thrust. The dimension parameter selected was the diameter instead of length, because defining the diameter will give an idea to the user of how much drag will be generated. Only one engine was considered for each stage, this was a simplification, because some launch vehicles have more than one engine in several stages, e.g. Proton.

Several Nose Cone geometries are available, 4 models were selected: Ogive, Power, Ellipse and Haack. This selection was purely mathematical, because as explained before was impossible to determine an analytical formula of drag for each nose cone. If the user takes the option to use Boosters, there is the possibility of choosing a different nose cone than the one chosen on the top of launcher. A detailed description is available in annex A.

Afterwards, in mass model the program will compare the masses obtained with heuristic equations i.e. Mass Estimation Relationships [Akin][1], and will iterate the structural ratio, until it converges.

During the mass model the program calculates in parallel the dimensions of the vehicle. The diameter of each stage is already defined. Then the volume is calculated and will iterate inside Mass Model. After the end of mass model all the masses and dimensions of the launcher are specified, the launcher is ready to trajectory simulations.

Then the trajectory has to be run, according to the three distinct phases of flight, firstly vertical flight, secondly gravity turn and then the free-flight phase, until the objective is fulfilled.

After knowing the best trajectory new values of ΔV drag and gravity and how much Propellant mass of the last stage remains or left, the program will transform those propellant in a ΔV, and then will iterate with those new values, regarding the Mass model.

The program will iterate until it finds a solution, i.e. when the ΔV used in the development of the launcher, are equal to the ΔV obtained in the trajectory and the payload reaches its objective with the right amount of propellant. The Launch Vehicle is optimized considering the initial objectives.

When the program is finished, a complete launcher has been developed, and its data can be tested for different objectives (Orbits and Payload).

In the figure 5.1 is represented the algorithm of the tool only for one combination of parameters and configuration. For each combination of these the tool will perform the algorithm described earlier and presented next. In the end, it will select the combination of parameters and configuration with minimum GLOW and maximum payload ratio.

[1] spacecraft.ssl.umd.edu

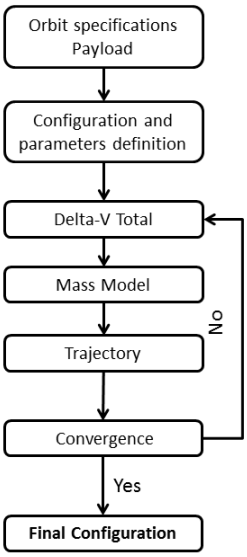

Figure 5.1: Algorithm for the Design of the rocket

5.3.1 Mass Model

The mass model of this tool was developed to calculate all the masses, dimensions and parameters of the rocket needed to perform the trajectory for each combination of parameters and configuration previously selected. When the mass model starts, the tool has already defined the parameters and the configuration. Those parameters will be used later for the Heuristics MERs.

For given stage velocities, the mass of the structure and propellants can be estimated using the ideal velocity equations, known as the Tsiolkovsky's Equation. The Lift-off weight is the sum of payload with all the calculated masses [55]. An initial estimate of the structural factor is used based on heuristics selected from database.

The structural and propellant mass of each stage are calculated with the following two equations:

$$m_{s_n} = \frac{\epsilon_n(k_n - 1)}{1 - \epsilon_n k_n} m_{pl}, \tag{5.1}$$

$$m_{p_n} = \frac{(k_n - 1)(1 - \epsilon_n)}{1 - k_n \epsilon_n} m_{pl}, \tag{5.2}$$

$$k_n = e^{\frac{\Delta V}{g I sp_n}}, \tag{5.3}$$

where ϵ_n and k_n are respectively the structural factor and the mass ratio for each stage.

The equations are used from top to bottom i.e., they start with the last stage, using payload mass, and for the subsequent stages the payload mass will be the sum of all rocket sections located above it.

Starting from the last stage, and knowing the initial structural factor, the mass ratio k_n and payload mass, it's possible to estimate the structural and propellant mass of that stage. Then a heuristic comparison is performed using the values generated (propellant and structural mass, volume of that stage) and

the parameters that are previously defined (thrust and nozzle area ratio). The Heuristic mass generated will provide a new structural factor, then the program iterates using this new value. The program will stop when the iteration of the structural factor converges with a maximum tolerance of 0.1%. This will define the last stage. Now, the program has the conditions to estimate the masses of next stage, where the mass of the payload will be the sum of masses of everything above. The same process is applied until all masses are defined. In the last stage, the model adds a percentage of the propellant calculated, for propellant reserve.

When the user chooses to use boosters during the first stage, there only is two solid propellants available. The user will select two ΔV, one for the "zeroth" stage considering the boosters and first stage burning simultaneously and one only for the first stage, after the boosters were discarded. Two is the minimum number of boosters to use and their burning time will be tested in the range 20% to 40% of the burning time of the first stage. After defining Thrust, with its burning time and the iteration of structural ratio, all the parameters are defined. A specific heuristic comparison for boosters is performed to validate the configuration.

In order to get appropriate dimensions for the Launcher, all the main dimensions are calculated. For each iteration of structural factor in mass model, a new propellant mass is generated. Knowing the density of propellant, we're in conditions to know the volume and calculate the involving structure for each stage. The volume of each stage will be $1.10 \cdot V_{tanks}$, the diameter for each stage is already defined so assuming a cylinder the length is calculated. Then, given a defined thickness for the structure and a density for the alloy, an estimate of the mass external structure of each stage is calculated and added to the heuristic structural mass [1].

$$M_{Struct} = \rho_{alloy} S th, \tag{5.4}$$

where ρ_{alloy} is the density of the alloy, S the surface Area, and th the thickness of the structure. The vehicle skin thickness must be as low as possible. A search for an heuristic of radius to wall thickness was made, but there isn't enough information available about this specific subject. The values of these parameters are resumed in the table below:

ρ_{alloy}	$2.7\ g/cm^3$
t	$33\ mm$

Table 5.2: Parameters of the Exterior Structure [2] [3].

The figure 5.2 shows the iterative process of how the mass model calculates the propellant and structural masses for each stage (rocket section mass), where the ΔV is the ΔV assigned for the specific stage.

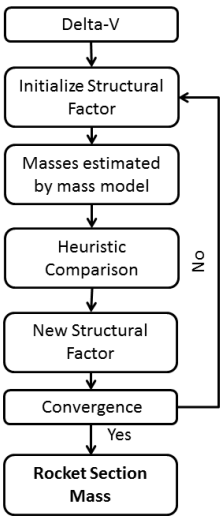

Figure 5.2: Mass model loop

5.3.2 Trajectory

For lift off, thrust level must exceed weight. The condition used is $(T/W > 1.2)$ [10], besides the convergence of the structural factor that's the other condition for exiting the mass model and entering the trajectory.

After the lift-off the launcher follows a vertical trajectory until a designed altitude where gravity turn starts. Although the altitude was fixed for running the simulations presented in this thesis, it can be changed and be a design parameter.

After the end of the gravity turn i.e. the end of the considerable atmosphere, the free-flight phase starts and the position and velocity of the vehicle is known, along with its destination (velocity and position). Considering the stages and respective thrust, the program will calculate how much burn time is necessary to achieve the desired orbit. Three different results can appear: arriving at a circular orbit at burnout, the most desirable one; burn time necessary is less than was previous calculated by the mass model; burn time is not enough to achieve the desired orbit. These cases still depend on the effective gravity and drag losses determined during the trajectory. If their values aren't correct the mass model will iterate until the both values converge.

In the first case, when the ΔV is the optimal solution, there is no need to perform any trade-off. If it is required to use this launcher with new objectives, the orbit and payload mass must be carefully selected, otherwise the launcher will probably fail.

The propellant mass missing or in excess in the last stage is converted to ΔV by Tsiolkovsky's equation. This will generate a new ΔV_{Total}. Then, the program will iterate until the value of ΔV converges with a tolerance of 0.01%.

When the program finishes, a complete launcher has been developed, and its data can be saved to try different orbits regarding that the maximum payload is the Payload used for initial design.

The figure 5.3 represents the trajectory part of the program, at the end of the mass model all the masses and burn times are defined based on a ΔV estimate, then the trajectory starts and the launcher ascents vertically until reaches a defined altitude, where the gravity turn starts, the end of this maneuver is defined by the Knudsen number equal to 5. When this maneuver ends starts the free-flight phase until the desired orbit, if the ΔV estimate is correct the final configuration is achieved, if not new value of ΔV estimate will iterate and the mass model will calculate new values for each mass and volume, then will enter the trajectory until the convergence.

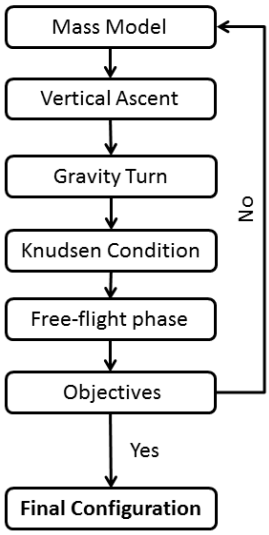

Figure 5.3: Trajectory

Chapter 6

Results

In this chapter a comparison of the results obtained by the program and with those provided by the user's manual was performed. Two different launchers were compared: Vega and Proton K. Posteriorly, a set of simulations was made, for the preliminary design and optimization of a new launcher, using as initial parameters the values of Ariane 5. The optimization was based on the variation of some of the original parameters and the result was a new launcher, an optimized Ariane 5.

6.1 Validation

Before using the tool for its purpose, its validation was necessary. It was performed in two separated phases, starting with the validation of the trajectory and ending with the validation of the mass model. The main objective of the simulation with Vega launcher was to place 1500 kilograms of payload into a circular orbit, at an altitude of 700 kilometres, and the main objective of the Proton K was to place 19360 kilograms of payload in a circular orbit at an altitude of 200 kilometres.

The procedures followed include, first, testing the trajectory, i.e. if it achieves the objectives proposed, and then running the entire program to compare the results obtained.

6.1.1 Trajectory

To validate the trajectory, firstly, a simulation was done with each launcher, using the specific characteristics (thrust, burn time, diameter, propellant and structural masses) of Vega and Proton K, to confirm if it managed to use the proposed trajectory. The principal characteristics of Vega launcher are presented in the table 6.1 and the principal characteristics of the Proton K/DM3 are presented in the table 6.2 .

-	1 Stage	2 Stage	3 Stage	4 Stage
Engine	P80	Zefiro 23	Zefiro 9	AVUM
Propellant Mass [kg]	88365	23906	10115	367
Structural Mass [kg]	7431	1845	833	418
Propellant	HTPB-Al/AP	HTPB/AP	HTPB/AP	Hydrazine/NTO
Isp [s]	280	289	294	317
Thrust [kN]	2092	959	230	2.2
Burn Time [s]	105	71	116	620
Diameter [m]	3	1.9	1.9	2.6
Nozzle Area Ratio	16	25	60.8	110

Table 6.1: *Vega Launcher - Main characteristics [4]*

Vega is an example of a newly developed small launcher. Initiated by the Italian Space Agency (ASI), Vega became an ESA development program. It's a three-stage solid propellant launch system with an orbit injection module using storable liquid propellants. It's launched from Guiana Space Center (CSG) near Kourou, French Guiana. After third stage separation at the sub-orbital trajectory, the multiple AVUM burns are used to transfer the payload to a wide variety of intermediate or final orbits, providing the required plane changes and the orbit raising.

-	1 Stage	2 Stage	3 Stage	4 Stage
Engine	RD-253 - 6	RD-0210 - 4	RD-0212	4 vernier RD-0214
Propellant Mass[kg]	419410	156113	46562	15200
Structural Mass[kg]	30590	11717	4185	3150
Propellant	UDMH/NTO	UDMH/NTO	UDMH/NTO	LOX/Kerosene
Isp[s]	316	289	327	353
Thrust	3492	2328	582	87
Burn Time	120	327	230	600
Diameter[m]	7.4	4.1	4.1	4
Nozzle Area Ratio	25	40	55	80

Table 6.2: *Proton K/DM3 - Main characteristics [5].*

Proton was, besides Ariane 5, the most important Launcher for lifting commercial payloads. Proton is a four-stage Launcher operated from the Baikonur launch site in Russia. The first three stages are propelled by storable liquids with identical engines that differ only in the length of their nozzle extensions. Alternatively, Block D with a semi-cryogenic propulsion system or the Breeze upper stage, which can be reignited up to 20 times, can be used as the fourth stage. Considering that the first stage has a non-usual configuration, the Drag model was maintained but to achieve more realistic results a new approach for Drag need to be applied for these configurations. In this simulation, Proton K don't use its upper stage DM-3. This simulation will assume the 4th stage as extra-Payload for re-insertion in other orbit.

After the lift-off the vehicle ascends vertically up to 500 meters where the gravity turn starts. This maneuver takes place until the effect of atmospheric conditions are negligible. To finish the GT and start the free-flight phase where TPBVP happens the launcher has to be in exo-atmospheric conditions, this means that the Knudsen number condition was achieved. The final times obtained at the end of the trajectory was lower than the sum of all burning and coast times, and in the last stage 34% and 38%

respectively of the propellant mass wasn't burned, meaning that the trajectory used was considered validated for this two launchers.

Many simulations of GT were run during the development of this work. It's possible to conclude that the gravity losses during Atmospheric flight are larger, in their maximum value, than the ones foreseen by the heuristics presented in chapter 4, that happens mainly because the launchers using this maneuver spend more time inside atmospheric conditions than the trajectories usually used by launchers. On the other hand the drag losses are smaller, this may occur by two conditions, the C_d model used produces underestimated results or the velocity of the launcher during the atmosphere is smaller than in the commonly trajectories.

6.1.2 Mass model validation

After the successful validation of the trajectory for each launcher. It's time to perform the validation of the mass model and of the entire tool.

The parameters introduced in the tool for the two simulations are presented in the table 6.3, all the parameters were equal as the ones presented in respective user's manual.

Characteristics	Units
Number of Stages	-
Number of Boosters	-
Nose Cone Selection	-
Diameter Booster	m
Diameter	m
Nozzle Area Ratio	m
Propellant Selection	-
Thrust	kN
Thrust Booster	kN
ΔV division	-

Table 6.3: Configuration and parameters introduced in the tool

Subsequently, if the mass model converge, the trajectory is used once again to search for improvements regarding the trajectory phase, i.e. reducing or increasing the propellant mass of the last stage, transforming this mass in ΔV value and iterate the new values of ΔV losses. As explained before, this change in the last stage mass will affect the other stages.

The total flight time was $357,4$ seconds and all the coast times are fixed to 3 seconds. The Knudsen number condition was achieved at 97.1 seconds where the Gravity Turn ends and then starts the free-flight phase.

The different variables, as propellant and structural mass, have been compared with the values presented in Vega User's Manual, and are presented in the table 6.4.

The expression used for the deviation of the results is

$$Deviation\% = \frac{|Theoretical - Simulated|}{Theoretical} \times 100, \tag{6.1}$$

where the theoretical values were obtained in the user's manual and the simulated ones with the tool.

	Stage 1			Stage 2			Stage 3			Stage 4		
	m_p [kg]	m_s [kg]	m_0 [kg]	m_p [kg]	m_s [kg]	m_0 [kg]	m_p [kg]	m_s [kg]	m_0 [kg]	m_p [kg]	m_s [kg]	m_0 [kg]
Vega	88365	7431	132530	23906	1845	36734	10115	833	10983	367	418	785
Simulation	83211.3	8595	126085	22918	2396.1	34248.9	8566.2	906.2	11663.8	516.6	175.6	2192.2
Deviation %	5.83	15.6	4.8	4.1	29.8	6.8	15.3	8.1	6.1	40.7	57.6	11.8

Table 6.4: *Mass Model Comparison - Vega*

The most significant differences were obtained in Structural mass, specially in the second stage where the difference was almost 30%. The structural and propellant mass of last stage are the ones that have more differences, specially the structural mass because last stage usually have "more structure", i.e. more avionics, wiring and a complicated thrust attitude controller for the re-ignitions, so the MERs used in Mass model doesn't have the same accuracy for upper stages as they have for lower stages.

The program overestimates all the structural masses but on the other hand the propellant masses calculated were inferior with the exception of the last stage once again, that can be explained by the fact that the last stage of the original launcher have multiple burns and long coast times and that analysis isn't provided in the trajectory. The difference in the others stages are explained for the non existence of the propellant margin. The biggest difference in the propellant masses excluding last stage was in third stage with a difference of 15.3%. The GLOW was a difference of 4.8%, that is inferior to 10% for a tool of preliminary design the differences are relatively small. The Payload mass was added to the last stage. The mass model was considered validated for this case.

The results of the dimensions achieved for the launcher are presented in the table 6.5.

	Stage 1			Stage 2			Stage 3			Stage 4		
	d $[m]$	l $[m]$	V $[m^3]$	d $[m]$	l $[m]$	V $[m^3]$	d $[m]$	l $[m]$	V $[m^3]$	d $[m]$	l $[m]$	V $[m^3]$
Vega	3	11.2	79.1	1.9	8.39	23.8	1.9	4.12	11.7	2.2	2	7.6
Simulation	3	10.6	74.9	1.9	8	22.7	1.9	3.7	10.5	2.2	1.5	6.7
Deviation %	-	5.4	5.3	-	4.6	4.6	-	10.2	10.3	-	25	11.8

Table 6.5: *Volume Comparison - Vega*

All the dimensions were inferior to the original Vega. That happens because the propellant masses of each stage were inferior compared with the original launcher, due to the definition of the total volume of each stage being an overestimation of the volume of the Propellant tanks. Although the difference in the volume, the effect in overall length is almost negligible.

A comparison between the flight performance/trajectory presented in the User's Manual, and the trajectory obtained by the code, was done. The results were considerably different, due to the fact that the trajectory uses a pure gravity turn and modern launchers now use powerful and effective guidance models. Also, the model assumes constant and maximum thrust in all stages but in real launchers, thrust isn't always at full power and sometimes, reverse thrust is used for the accommodation of payload and astronauts.

The following figures show different variables of the trajectory simulation. Only in two are represented

all the parts of flight. In the other figures, it's more difficult to see the first phase of the flight, it's only possible to observe the second and third phases. The Gravity Turn ends when the flight time was 97.1 seconds and after that the launcher starts to raise faster to the desired orbit. The total flight time was 357.4 seconds.

In the figure 6.1 its presented the evolution of the Altitude with time, after the end of GT the launcher starts to accelerates and velocity increases. In the figure 6.1 its presented the evolution of the altitude vs downrange of the trajectory.

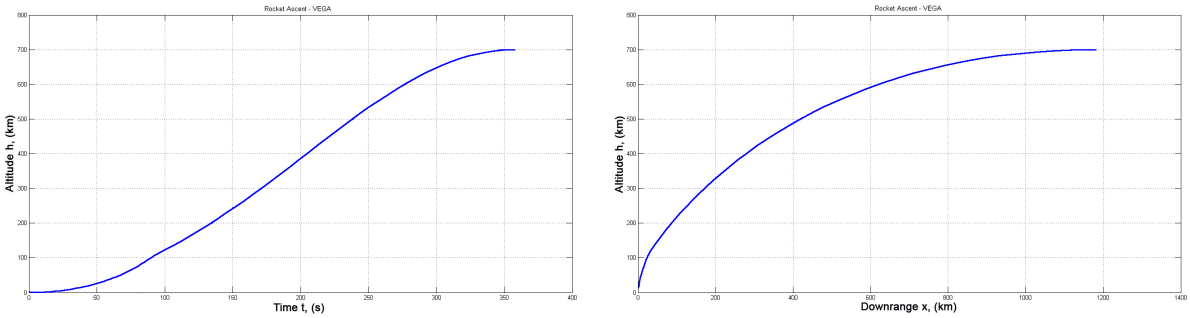

(a) Altitude vs Time - Vega

(b) Altitude vs Downrange - Vega

Figure 6.1: *Vega Launcher Simulation*

It's possible to observe, in fig 6.2(a) the Flight Path Angle, divided in three separate phases, first the vertical ascent phase where the FPA doesn't change, second gravity turn and then the free-flight phase. In the figure 6.2(b) it's possible to observe the velocity function of time and the change after the end of gravity turn.

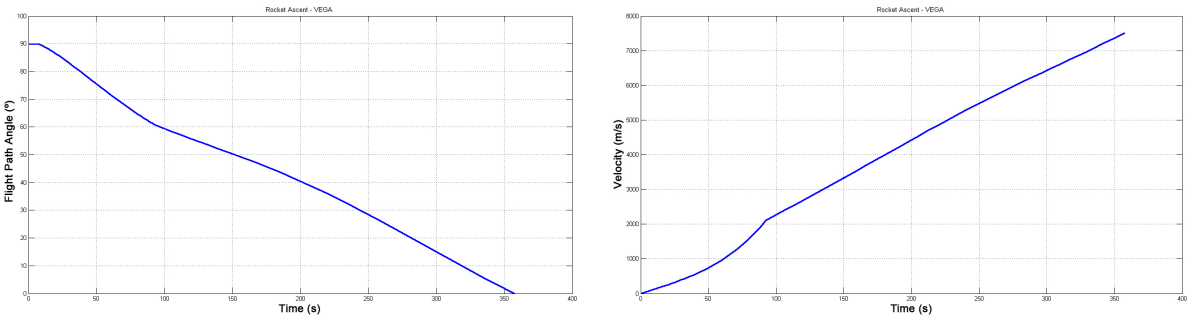

(a) Flight Path Angle vs Time - Vega

(b) Velocity vs Time - Vega

Figure 6.2: *Vega Launcher Simulation*

In the figure 6.3(a) is represented the Altitude as a function of Velocity, where is possible to observe the end of GT and the start of the free-flight phase. In the figure 6.3(a) the Dynamic Pressure is represented. This value is very important in the design phase for Structural strength and reliability of Fairing during the first part of the trajectory. The maximum occurs around 9 km of altitude, that was assumed correct because the maximum usually occurs around an altitude of 10 km.

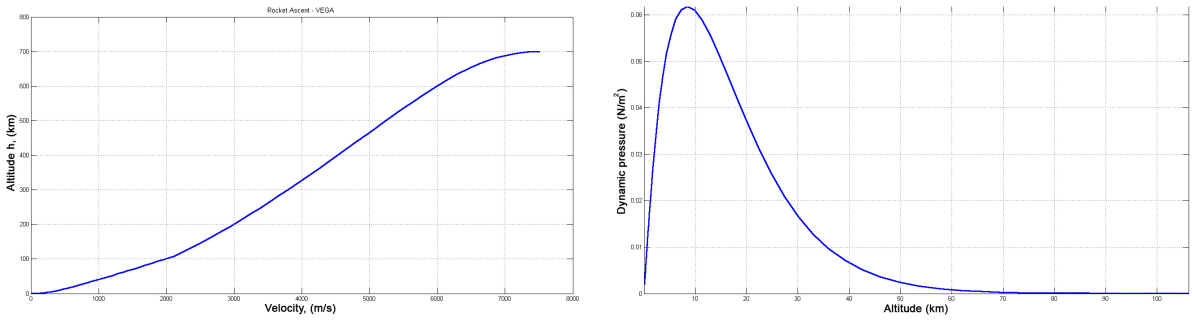

(a) Altitude vs Velocity - Vega

(b) Dynamic Pressure - Vega

Figure 6.3: *Vega Launcher Simulation*

After the validation of the mass model and the tool with the small launcher Vega, we proceed with the simulations with Proton K launcher.

The parameters used to input in the program were the same as in Vega simulation, they are presented in the table 6.2.

The total flight time to orbit was 509.2 seconds. The two coast phases are equal to Vega simulation, 3 seconds each. The Gravity Turn starts at an altitude of 500 meters. The altitude where the free-flight phase started was higher than the Vega simulation because the diameter of last stage of Proton is higher than the Vega, which means that Proton needs to raise higher to achieve exo-atmospheric conditions defined by Knudsen Number.

The mass model results are presented in table 6.6.

	Stage 1			Stage 2			Stage 3		
	m_p [kg]	m_s [kg]	m_0 [kg]	m_p [kg]	m_s [kg]	m_0 [kg]	m_p [kg]	m_s [kg]	m_0 [kg]
PROTON K	419410	30590	668577	156113	11717	218577	46562	4185	50747
Simulation 1	395390	36563	626563	142878	12323	194610	34127	5282	39409
Deviation %	5.7	19.5	6.3	8.5	5.2	11	26.7	26.2	22.3

Table 6.6: *Mass Model Comparison - PROTON K*

Once again, the mass variables are compared between the user's manual information and the results obtained by the tool. All the propellant masses calculated were inferior than the original Launcher, being the biggest difference in the last stage and the smallest in the first stage. The differences are explained by the non existence of the propellant margin. The structural mass calculated was always superior than the real Launcher: the biggest difference was in the last stage and the smallest was in the second stage. The GLOW had a difference of 6.2%. For a tool of preliminary design the differences are relatively small and the mass model was considered validated for this case.

All the dimensions results are presented in table 6.7.

The values were inferior compared with Proton K original, because the propellant masses of each stage were inferior compared with the original Launcher and the definition of the total volume of each stage is an overestimation of the volume of the propellant tanks. The differences in the Volume are larger in upper stages being around 24%, but the effect in overall length is, once again, almost negligible.

	Stage 1			Stage 2			Stage 3		
	d $[m]$	l $[m]$	V $[m^3]$	d $[m]$	l $[m]$	V $[m^3]$	d $[m]$	l $[m]$	V $[m^3]$
Proton K	7.4	21.2	911.3	4.1	14.39	190	4.1	6.5	85.8
Simulation	7.4	20.1	864	4.1	13.3	175.5	4.1	4.9	64.7
Deviation	-	5.2	5.2	-	7.6	7.6	-	24.6	24.6

Table 6.7: *Volume Comparison - Proton K*

A comparison between the trajectory obtained by the code and the flight performance/trajectory presented in the Users Manual can't be performed because the flight performance wasn't available in the user's manual.

The following figures show different variables of the trajectory simulation. Only in two figures all the parts of flight are represented. In the other figures, it's more difficult to see the first phase of the flight, it's only possible to observe the second and third phases. The Gravity Turn ends at 153 seconds and after that the launcher starts to raise to the desired orbit. The total flight time was 509.2 seconds. Here, the payload achieves its desired orbit with 5% of propellant reserve.

In figure 6.4(a) its represented the Altitude of the trajectory vs time. In the figure 6.4(b) is represented the altitude vs downrange, it's possible to observe in both figures that the payload reaches the desired orbit.

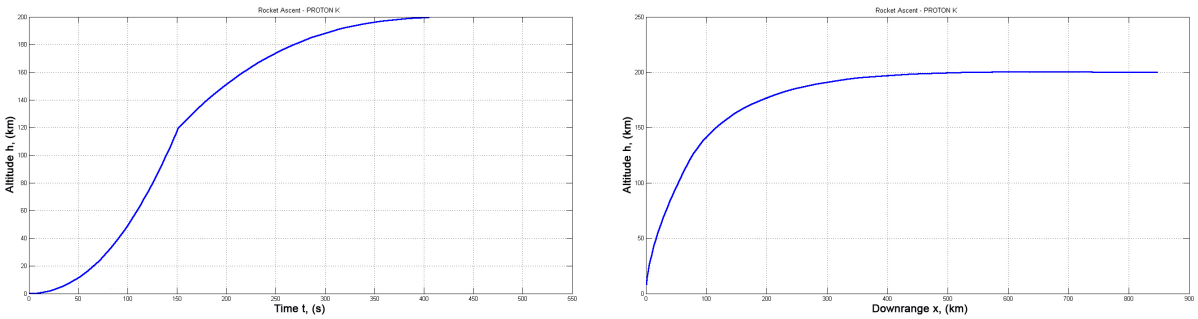

(a) Altitude vs Time - Proton K

(b) Altitude vs Downrange - Proton K

Figure 6.4: *Proton K Launch Simulation*

In the figure 6.5(a) its represented the Flight Path Angle vs time, divided in three distinct phases, first the vertical ascent, then Gravity Turn until the end of considerable atmosphere and at last the free-flight phase until the desired orbit. The figure 6.5(b) represents velocity of Launcher vs time, where it's also possible to observe the end of GT and the start of the free-flight phase and how the launcher rapidly ascents to the desired orbit.

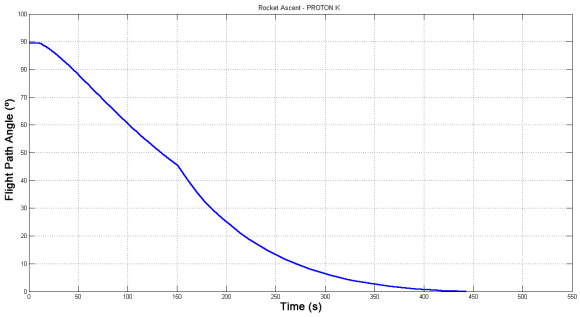

(a) Flight Path Angle vs Time - Proton K

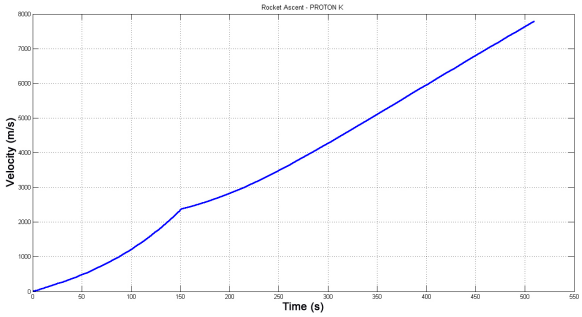

(b) Velocity vs Time - Proton K

Figure 6.5: *Proton K Launch Simulation*

In the figure 6.6(a) is represented the evolution of velocity with the altitude, where once again it's possible to observe the two principal phases of the trajectory, the end of GT and the start of the free-flight phase around an altitude of 120 km. In the figure 6.6(b) its presented the Dynamic pressure felt from the vehicle in the first phases of flight and is importance has explained before.

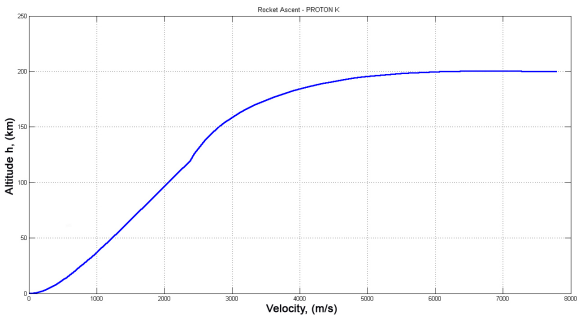

(a) Altitude vs Velocity - Proton K

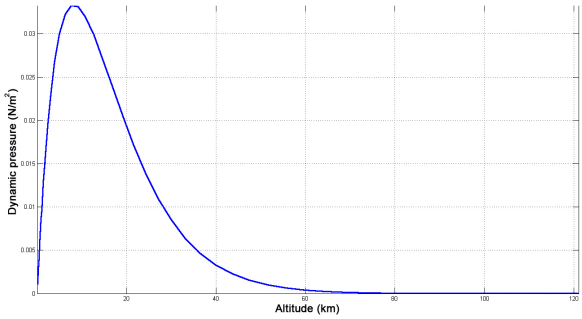

(b) Dynamic Pressure - Proton K

Figure 6.6: *Proton K Launch Simulation*

6.2 Preliminary Design and Optimization

In the last case, a set of simulations was done with the objectives of Ariane 5 for LEO, an altitude of 200 km and a payload mass of 19.3 tons, but in this simulation some parameters were varied with the goal of obtaining an optimal configuration, this means the minimum GLOW that can satisfied the desired objectives.

The Ariane 5 is a 2.5-stage launch system primarily used for lifting heavy satellites to a GTO. Its capability of launching two satellites totalling a maximum of 9 tons to GTO and 18 tons to LEO. Two versions are operated today: A5E/CA with a cryogenic upper stage for launching commercial payloads and A5ES-ATV for lifting the ATV supply vehicle to the ISS. The upper stage of this version is re-ignitable and uses storable liquid propellants. Both versions use a cryogenic first stage and two large solid propellant boost stages. Ariane 5 is launched from the European CSG spaceport near Kourou in French Guiana.

The principal characteristics of the Ariane 5 are presented in the table 6.8.

-	**Boosters**	**1 Stage**	**2 Stage**
Engine	EAP	EPC 23	ESC-A
Propellant Mass [kg]	480000	170000	14900
Structural Mass [kg]	80000	14700	4540
Propellant	$HTPB - Al/AP$	$LOX + LH_2$	$LOX + LH_2$
Isp [s]	274.5	432	446
Thrust [kN]	14000	1390	67
Burn Time [s]	129	537	972
Diameter [m]	3	5.4	5.4
Nozzle Area Ratio	30	57	88

Table 6.8: *Ariane 5 Launcher - Main characteristics.*

Three groups of different simulations were run. In the first group, the diameter and thrust of each stage were fixed but on the other hand the number of boosters and its characteristics, thrust, diameter and burn time were varied in a certain range. In parallel with the first group simulation, the second group simulation was run with all the parameters fixed except the diameter of core stages. The third group simulation used the best result of the first group simulation for the boosters (its thrust and dimensions) and the best diameter obtained in the second group simulation with the variation of ΔV division and respective thrust for each stage. In the end, an optimal solution was found and its configuration was the one with minimum GLOW that achieves the objectives early proposed. A total of 170 simulations were run and a total of seven parameters were varied and its variation it's represented in the table 6.9.

Parameters	Range of Values	Number of points
Diameter [m]	$5.4 \pm 36\%$	11
Thrust [kN]	$\pm 25\%$	5
$\Delta V division$	$[20\%\ 50\%\ 30\%] \pm 5\%$	23
Number of boosters	0-2	2
Thrust booster [kN]	± 14 %	3
Diameter booster [m]	$3.05 \pm 25\%$	5
Burn time Booster [%]	$30\% \pm 10\%$	5

Table 6.9: Parameters varied in the tool.

In the first group of simulations, three parameters were varied: the number of boosters, the thrust level of each booster and the burn time duration of the boosters compared to the burn time of first stage. First, a simulation without boosters was run, then using boosters and varying their burn time and thrust. The results obtained showed that the use of boosters in heavy lift launchers provided an increment of total payload ratio and at the same time the decrease of the GLOW. The simulations without the use of boosters results in a GLOW 10% heavier, compared with the ones using the boosters.

The maximum value of thrust was selected because the increment of dry weight in booster was lower than the propellant saved in last stage, the diameter selected was the second lowest because the lowest one besides giving the lowest GLOW, has more length than the first stage and that is a condition that cannot be exceeded. The burn time of booster that achieves lowest GLOW was the second minimum value, 25% of the burn time of the first stage. This result was equal to the original Ariane 5, that means the boosters work better in the first phases of flight and after that phase need to be discarded.

The second group of simulations has the objective of finding the best diameter that achieves minimum GLOW with the rest of the parameters of Ariane 5 fixed. In the trajectory, the diameter is a key parameter that defines when the forces of atmosphere can be neglected and then starts the free-flight phase, so the simulations with lower diameters will start the free-flight phase earlier in altitude and the optimized trajectory will achieve best results. This happens because free-flight phase is more efficient than Gravity Turn, allows to save propellant mass in last stage and has lower values in Drag because it only considers the cross sectional area, neglecting the skin friction depending of the Length of the vehicle. The best result was achieved with the lowest value of diameter, however this result must be carefully used because buckling problems. Structural analysis wasn't developed in this study.

The third group simulation already used the results generated by the first and second group simulations and the parameters varied were the thrust and ΔV assigned for each stage. The best configuration was achieved with the second lowest thrust level of second stage because often in the upper stages the dry mass is relatively high, so reducing the thrust will reduce the weight of the engine and thrust structure was lower reducing the GLOW. On the other hand, in lower stage the thrust selected was the higher one, that means in the first phases of flight the thrust must be the higher value possible to quickly leave the atmosphere but paying attention to increase of drag forces. The variation of ΔV assigned to each stage provided interesting results. Increasing the ΔV assigned to Booster and second stage and decreasing for the first stage.

The objective was to optimize an existing launcher and not to validate the code, the objective wasn't

to see if the results match but how different will be the new optimized launcher compared with the original Ariane 5, how lighter will be, and how the volume will vary. The values achieved for the best configuration are presented in the table 6.10.

Parameters	Final Value
Diameter [m]	3.9
Thrust [kN]	1700 and 58.5
$\Delta V division$ [%]	[25% 49% 26%]
Number of boosters	2
Thrust booster [kN]	8000
Diameter booster [m]	2.625
Burn time Booster [%]	25%

Table 6.10: Optimal Configuration Achieved.

The total flight time to orbit was 462.8 seconds. The coast phase is equal to Vega and Proton K simulation, 3 seconds. The Gravity Turn starts at an altitude of 500 meters. The altitude where the free-flight phase started was higher than the Vega's and almost the same altitude of the Proton K's simulations because the diameter of last stage simulated was 3.9 meters, meaning that the optimized launcher needs to raise up to 120 kilometres to achieve exo-atmospheric conditions.

First, the different masses are compared between the user's manual information and the results obtained by the last simulation. The results are presented in the table 6.11.

	Booster			Stage 1			Stage 2		
	m_p [kg]	m_s [kg]	m_0 [kg]	m_p [kg]	m_s [kg]	m_0 [kg]	m_p [kg]	m_s [kg]	m_0 [kg]
Ariane 5	480000	80000	764140	170000	14700	204140	14900	4540	19440
Simulation	458189.4	77216	680076.5	123735	14406	144671.1	2217	4313	6530
Deviation %	4.5	3.5	11	27.2	2	29.1	85.1	5	66.4

Table 6.11: *Mass Model Comparison - Ariane 5*

In this optimization all the propellant masses calculated were smaller than the ones from the original Launcher, the biggest difference being in the last stage and the smallest around in the booster stage. Comparing this differences, with those obtained for the validations of the model it's possible to state that optimization of the parameters decrease the propellant necessary to achieve the orbit. The structural masses calculated were slightly inferior than the ones from the real Launcher: the biggest difference was in the second stage and the smallest happened in first stage. These difference can be explained by the reduction of the mass of the propellant and its direct influence in decreasing the mass of the propellant tanks.

The goal of this optimization was the reduction of GLOW, the final simulation had a difference of 11%, which allows to reduce 84 tons the weight of the Launcher at lift-off and compared with the other simulations, where the objective was to validate the code, it possible to say that the original Ariane 5 was optimized and consequently its GLOW reduced.

The dimensions obtained are presented in the table 6.12. The values were inferior compared with Ariane 5 original because the propellant masses of each stage were inferior due to optimization.

	Booster			Stage 1			Stage 2		
	d $[m]$	l $[m]$	V $[m^3]$	d $[m]$	l $[m]$	V $[m^3]$	d $[m]$	l $[m]$	V $[m^3]$
Ariane 5	3.05	31.6	230.75	5.4	30.5	698.16	5.4	4.71	107.81
Simulation	2.62	36.99	199.37	3.9	54.44	638.16	3.9	7.43	88.73
Deviation %	14.1	17.1	13.6	27.8	44	8.6	27.8	36.6	17.7

Table 6.12: *Volume Comparison - Ariane 5*

The differences are higher in upper stage because that was the stage that had more propellant reduction. The overall length was 3.1 meters higher than original Ariane 5, increasing 5.5% the total length of the Launcher. One way to keep all dimensions low is a high thrust-to-weight ratio, however it would increase the Drag loss as explained in Chapter 4.

The following figures show different variables of the trajectory simulation. The gravity turn ends at 111.5 seconds at an altitude of $h = 120.4$ kilometres of altitude and after that the launcher starts to raise faster into the desired orbit. The total flight time was 462.8 seconds.

In the figure 6.7(a) is represented the altitude of the trajectory vs time, where it's possible to observe the end of GT and the start of the free-flight phase. In the figure 6.7(b) is represented the altitude vs downrange, where it's difficult to observe the end of GT and the start of the free-flight phase but it occurs at an altitude of 120 kilometres and with a closer look it's possible to observe a slightly change in the attitude. In both figures it's possible to observe that the payload reaches the desired orbit at burnout.

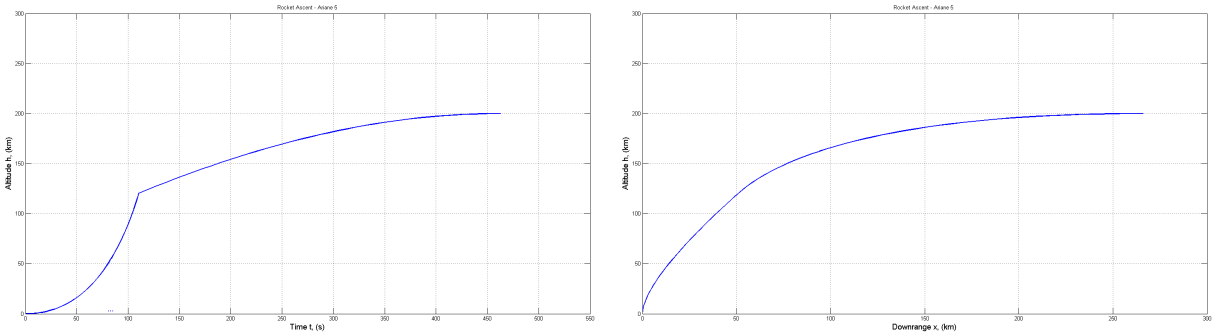

(a) Altitude vs Time - Ariane 5

(b) Altitude vs Downrange - Ariane 5

Figure 6.7: Ariane 5 Launch Simulation

In the figure 6.8(a) its represented the Flight Path Angle vs time, divided in three distinct phases, vertical ascent, then GT until the end of considerable atmosphere and then the free-flight phase starts, this transition occurs at $\gamma = 58.9^{\circ}$ where it's possible to observe the difference. The figure 6.8(b) represents the velocity of Launcher vs time, where it's possible to observe the end of GT and the start of the free-flight phase when the velocity raises slowly in beginning, accelerating then until the desired orbit.

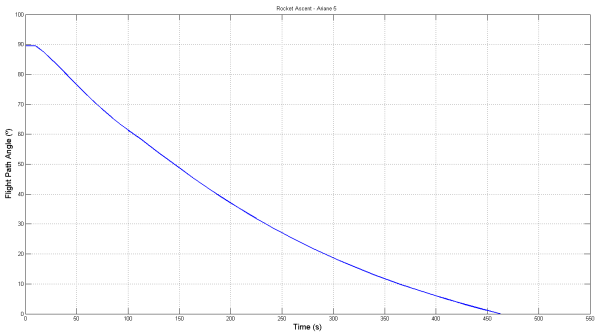

(a) Flight Path Angle vs Time - Ariane 5

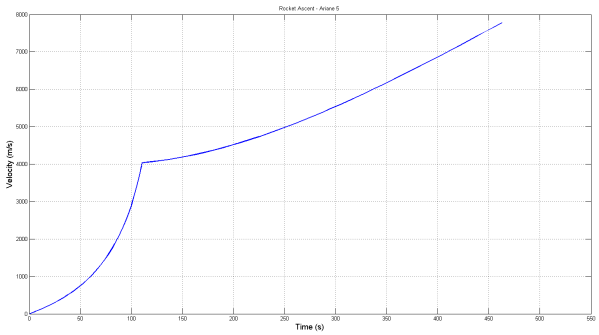

(b) Velocity vs Time - Ariane 5

Figure 6.8: Ariane 5 Launch Simulation

In figure 6.9(a) are represented the evolution of the velocity with the altitude, where it's possible to observe the launcher had difficulties to gain velocity in the first phases of flight, due to dense lower atmosphere, raising then until the end of GT and the start of the free-flight phase. In the figure 6.9(b) is represented the Dynamic pressure felt from the vehicle in the first phases of flight.

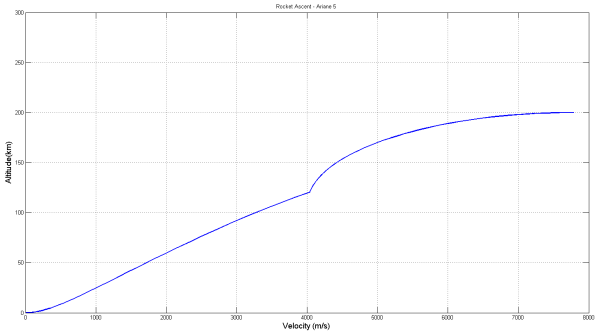

(a) Altitude vs Velocity - Ariane 5

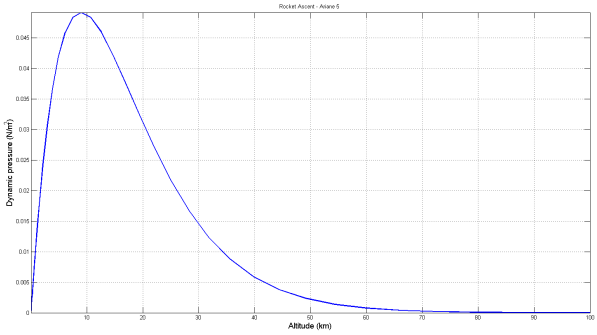

(b) Dynamic Pressure - Ariane 5

Figure 6.9: Ariane 5 Launch Simulation

Chapter 7

Conclusions

The main goal of this research was to develop a tool to assist the preliminary design of rockets. The tool was modelled using a MATLAB code, which applies a simplified optimization, and covers two major fields: the mass model and the trajectory.

The database created during this study allowed the understanding of some important variables, such as length, diameter, thrust, burning time, specific masses and others, providing their range of values and ensuring the viability of the final result. Some of these values were used in the mass model, as initial structural factors, for the iteration of the mass model, such as the fairing mass, estimated from GLOW and the respective volume, to accommodate the payload. An effort to create MERs was done, but the lack and dispersion of information available about the specific mass of the components, made this estimation almost impossible to perform. Nonetheless, MERs were estimated, concerning fairing.

The mass model created, showed that the use of Tsiolkovsky's equation with the MERs heuristics, provides realistic results for the structural masses of the launcher. The structural factor iterates until it finds convergence with the MERs heuristics and the design is made from top to bottom. This model also calculates the dimensions of the launcher, with the goal of adding more realism to the final design; the weight of the external structure of each stage is estimated by the definition of volumes. When the mass model is concluded, all the masses needed for the trajectory model (propellant and structural mass) and dimensions of the launcher have been defined. This is important, because the diameter of the last stage is one of the conditions to define the Knudsen number.

The trajectory was divided into three distinct phases. Initially, after the lift-off, the launcher rises vertically until a certain altitude, the value used for the simulations was 500 m, but it can be optimized. After this, it starts the gravity turn, which ends when the atmosphere affects are negligible, condition defined by the Knudsen number. When the launcher achieves exo-atmospheric conditions, it starts the free-flight phase, which will minimize the time, and consequently, the propellant used. The atmospheric model used is a combination of the US standard atmosphere of 1962 and 1976 valid up to an altitude of 2000 kilometres. A simplified drag model was used, where the C_d only varies with Mach number. The same happens for gravity model where the gravity only varies with altitude.

When the program is concluded, a new Launcher has been designed and all the masses and di-

mensions have been defined. In this phase, new objectives can be tested, taking into account that the maximum payload is the designed one and that the orbits must be carefully selected.

The Model validation is important to determine the accuracy of the results obtained. In this study, the model validation was done regarding two examples, Vega and Proton K, targeting different objectives (Orbit and Payload Mass) and characterised by different configurations. Both validations were done with the values presented in the user's manual. First, an isolated simulation of the trajectory was done, i.e. using the mass values from the user's manual, the launcher achieves the desired objectives. Both simulations were successful, achieving the desired orbit with some propellant mass of the last stage in their tanks. The difference between both results and their user's manual can be explained by the assumption of constant and maximum thrust in every stage and for the completely burnout of the propellant mass assumed in the tool, which doesn't correspond to the real way launchers operate.

After the validation of the trajectory, it was possible to validate the mass model. All the parameters selected for the design were fixed and were the same of the respective User's manual. The results showed that almost all the propellant masses were inferior, when compared to real launchers, explained by the fact that the mass model only adds propellant margin for the last stage, instead of adding it for all stages. The structural masses were almost all superior, when compared with real launchers, meaning the mass model is over estimating the structural weight for the selected launchers. The GLOW of each launcher was inferior, and that is explained by the reasons presented for the deviation regarding the propellant masses. Almost all the dimensions were inferior compared to the user's manual, because of the dependency of the total volume of the propellant mass, since the densities of the propellants were the same.

After the validation of the developed tool, this was used for the preliminary design of a rocket. The original parameters used were based on launcher Ariane 5, and some were modified, to optimize the rocket i.e. increase the payload ratio by reducing the GLOW. This allowed the understanding of which parameters influence more the difficult task of designing a rocket. The objectives of the mission were the same as those defined for Ariane 5 (orbit and payload mass) and in the end of the optimization all masses and dimensions were compared with the user's manual. All the masses were inferior; the propellant masses differences can be explained by the non-existence of propellant margin and also by the reduction of the diameter, which allowed the free-flight phase to start earlier; the structural masses were also inferior because of the reduction of all propellants masses, the lighter tanks and the reduction of the diameter, which decreased the weight of the structure and allowed the free-flight phase of the trajectory to start earlier, optimizing the fuel consumption. In conclusion, the reduction of GLOW was significant, meaning that the optimization was successful.

The ΔV division and thrust are the parameters that most influence the GLOW. The definition of diameter effects drag and trajectory because of the definition of the Knudsen number and must be carefully selected, due to the fact that in this study a structural analysis wasn't developed. The use of boosters increased the payload ratio, i.e. the payload mass increases for the same GLOW, and this effect is more significant in medium and heavy launchers. The burning time of boosters must be reduced to allow a rapid discard of the mass of its empty tanks.

As a conclusion, a tool to assist the design, and improve the configuration of a space launch vehicle, was created. Its validation was done comparing the results obtained with Vega and Proton K launchers. The results indicate that the program can be used as a starting point in the difficult task of designing earth launch vehicles. The set of simulations performed with Ariane 5 demonstrated that this tool can also be used as an optimizer, for already existing configurations. By varying some parameters it is possible to obtain a whole new configuration, for the objectives earlier defined.

7.1 Future Work

Below are presented some ideas for future developments, to allow further studies on this subject.

- Implement a Guide User Interface (GUI), that will allow users to run the program without requiring knowledge of the language of the code.
- Include the chamber pressure and the Nozzle areas in the Mass model. Currently its effect is neglected on the nozzle mass, defining the pressure at exit to improve the thrust model with Nozzle Area Ratio.
- Implement a more realistic Mass model for the engine. If mass only depends on Thrust, i.e. if the engine increases its efficiency, its mass will also increase.
- Improve the Drag model. A more realistic Drag model can be achieved with analytical equations for each Nose Cone Configuration. The use of other Software like DATCOM cannot be discarded.
- Implement constrains in the Trajectory model, such as Max. Dynamic Pressure, Heat Flux, Bending Load and Axial Acceleration. Some of this values are already calculated in the program, so a thrust vector control have to be created. This will provide a more realistic trajectory.
- Develop more options for Boosters, defining various types of Grain Geometry, special nose cones and increase the available solid propellants used in the Code.
- Implement some changes to air launched rockets (Pegasus) and to those launched with inclination, for safety reasons, like in Japan.
- Develop a Cost Model, or use an existing one, in order to obtain a realistic insight of Launch Vehicle Design.
- Design transfer orbits to GEO and interplanetary trajectories, with the improvement of the Guidance Model to perform long Coast Phases.
- Include dis-alignment Thrust vector in $\Delta V Losses$, the effect of the Earth's non-spherical gravitational field and the effect of gravity from other bodies (Moon and Sun).
- Rewrite the program in C or C++ will decrease the time necessary to complete the simulations.

Bibliography

[1] George P. Sutton. *Rocket Propulsion Elements*. 8 edition, 2010.

[2] Willi Hallmann Klaus Wittmann and Wilfried Ley. *Handbook of Space Technology*. Wiley, 2009.

[3] NASA. *Space Shuttle User's Manual*, 2008.

[4] Arianespace. *VEGA User's Manual*, 2006.

[5] *PROTON Launch System Mission Planner's Guide*, 2001.

[6] National Aeronautics. Rockets - A Teacher's Guide, 1999.

[7] Frank H. Winter, Michael J. Neufeld, and Kerrie Dougherty. Was the rocket invented or accidentally discovered? Some new observations on its origins. *Acta Astronautica*, 77:131–137, August 2012.

[8] Alan C. Tribble. *A Tribble's guide to Space*. Princeton, 2000.

[9] Jim Winchester. *Space Missions*. Amber, 2006.

[10] Willam E. Wiesel. *Spaceflight Dynamics*. Aphelion, third edition edition, 2010.

[11] E. Civek-Coskun and Kemal Ozgoren. A generalized staging optimization program for space launch vehicles. *Recent Advances in Space Technologies (RAST)*, pages 857–862, 2013.

[12] Reza Jamilnia and Abolghasem Naghash. Simultaneous optimization of staging and trajectory of launch vehicles using two different approaches. *Aerospace Science and Technology*, 23(1):85–92, 2012.

[13] R D Braun and A A Moore. Collaborative Approach to Launch Vehicle Design. *Journal of Spacecraft and Rockets*, 34(4), 1997.

[14] Amer Farhan Rafique, He LinShu, Ali Kamran, and Qasim Zeeshan. Multidisciplinary design of air launched satellite launch vehicle: Performance comparison of heuristic optimization methods. *Acta Astronautica*, 67(7-8):826–844, October 2010.

[15] Lawrence F Rowell, Robert D Braun, and John R Oldst. Multidisciplinary Conceptual Design Optimization of Space Transportation Systems. *Journal of Aircraft*, 36(1), 1999.

[16] Mathieu Balesdent, Nicolas Bérend, Philippe Dépincé, and Abdelhamid Chriette. A survey of multidisciplinary design optimization methods in launch vehicle design. *Structural and Multidisciplinary Optimization*, 45(5):619–642, September 2011.

[17] R. D. Braun, R. W. Powell, R. a. Lepsch, D. O. Stanley, and I. M. Kroo. Comparison of two multidisciplinary optimization strategies for launch-vehicle design. *Journal of Spacecraft and Rockets*, 32(3):404–410, May 1995.

[18] Young Chang Choi, Kyung-Ho Noh, Jae-Woo Lee, Yung-Hwan Byun, and Bong-Kyo Park. Optimal air-launching rocket design using system trades and a multi-disciplinary optimization approach. *Aerospace Science and Technology*, 13(7):406–414, October 2009.

[19] Rizwan Ullah, De-qun Zhou, Peng Zhou, Mukarrum Hussain, and M Amjad Sohail. An approach for space launch vehicle conceptual design and multi-attribute evaluation. *Aerospace Science and Technology*, 25(1):65–74, 2013.

[20] David R. Greatrix. *Powered Flight - The Engineering of Aerospace Propulsion*. Springer, 2012.

[21] Fernando Alonso Zotes and Matilde Santos Peñas. Multi-criteria genetic optimisation of the manoeuvres of a two-stage launcher. *Information Sciences*, 180(6):896–910, March 2010.

[22] Emanuele Di Sotto and Paolo Teofilato. Semi-Analytical Formulas for Launcher Performance Evaluation. *Journal of Guidance, Control, and Dynamics*, 25(3), 2002.

[23] Ping Lu and Binfeng Pan. Highly Constrained Optimal Launch Ascent Guidance. *Journal of Guidance, Control, and Dynamics*, 33(2):404–414, March 2010.

[24] Nicolas Berend and Christophe Talbot. Overview of some optimal control methods adapted to expendable and reusable launch vehicle trajectories. *Aerospace Science and Technology*, 10(3):222–232, April 2006.

[25] Greg A Dukeman, Nasa Marshall, Space Flight, and Ashley D Hill. Rapid Trajectory Optimization For the ARES I Launch Vehicle. Technical Report August, 2008.

[26] D. M. Azimov. Active Rocket Trajectory Arcs: A Review. *Automation and Remote Control*, 66(11):1715–1732, November 2005.

[27] John T. Betts. Survey of Numerical Methods for Trajectory Optimization. *Journal of Guidance, Control, and Dynamics*, 21(2):193–207, March 1998.

[28] E. Trélat. Optimal Control and Applications to Aerospace: Some Results and Challenges. *Journal of Optimization Theory and Applications*, 154(3):713–758, April 2012.

[29] Max Cerf, Thomas Haberkorn, and Emmanuel Trélat. Continuation from a flat to a round Earth model in the coplanar orbit transfer problem. *Optimal Control Applications and Methods*, 2011.

[30] Takeshi Tsuchiya. Optimal Conceptual Design of Two-Stage Reusable Rocket. *Journal of Spacecraft and Rockets*, 41(5), 2004.

[31] Michael Thierschmann. SSTO applications based on super high energy propulsion systems. *Acta Astronautica*, 22:219–227, 1990.

[32] H.D. Froning Jr and Huntington Beach. Investigation of very high energy rocket for future SSTO vehicles. *Acta Astronautica*, 19(4):321–330, 1989.

[33] Dietrich E. Koelle. Economics of Small fully Reusable Launch Systems. *Acta Astronautica*, 40(2):535–544, 1991.

[34] Martin J. Bayer. Analytic performance considerations for lifting ascent trajectories of winged launch vehicles. *Acta Astronautica*, 54(10):713–721, May 2004.

[35] Ashish Tewari. *Atmospheric and Space Flight Dynamics*. Birkhauser, 2006.

[36] Claire Ballard. Conceptual Lay-out of a Small Launcher. Master's thesis, 2012.

[37] Jack D Mattingly and Hans Von Ohain. *Elements of Propulsion : Gas Turbines and Rockets*. AIAA, 2006.

[38] Joseph Z. Ben-Asher. *Optimal Control Theory with Aerospace Applications*. 2010.

[39] Sighard F. Hoerner. *Fluid-Dynamic Drag*. Hoerner Fluid Dynamics, 1965.

[40] Ashish Tewari. *Advanced Control of Aircraft, Spacecraft and Rockets*. Wiley, 2011.

[41] American Institute of Aeronautics and Astronautics. American National Standard Guide to Reference and Standard Atmosphere Models. Technical report, 2009.

[42] Eurockot. *Rockot User's Guide*, 2011.

[43] Orbital. *Pegasus User's Guide*, 2007.

[44] SpaceX. *Falcon 1 Launch Vehicle Payload User ' s Guide*, 2008.

[45] Arianespace. *SOYUZ User's Manual*, 2006.

[46] SLLP. *Zenit User's Guide*, 2000.

[47] United Launch Alliance. *Delta IV Launch Services User's Guide*. United Launch Alliance, 2013.

[48] Arianespace. *Ariane 5 User's Manual*, 2011.

[49] United Launch Alliance. *Atlas V Launch Services User's Guide*. United Launch Alliance, 2010.

[50] B. T. C. Zandbergen. AE1222-II : Aerospace Design Systems Engineering Elements I Part : Launcher design and sizing .

[51] Reuben R Rohrschneider. Development of a Mass Estimating Relationship Database for Launch Vehicle Conceptual Design. Technical report, 2002.

[52] Willie Heinemun Jr. NASA Technical Note fundamental techniques of weight estimating and forecasting for advanced manned spacecraft and space stations. Technical Report May, 1971.

[53] P.J. Klich. NASA Technical Memorandum of Mass Properties of Earth-To-Orbit Transportation Systems. Technical report, 1978.

[54] Francesco Castellini. *Multidiscplinary Design Optimization for Expendable Launch Vehicles*. PhD thesis, Politecnico di Milano, 2012.

[55] Geethaikrishnan. Multi-Disciplinary design optimization strategy in multi-stage launch vehicle conceptual design,. *Department of Aeroespace Engineering Indian Institute of Technology*, 2003.

[56] W. T. Thomson. *Introduction to Space Dynamics*. Dover, 1986.

[57] Howard Curtis. *Orbital Mechanics for Engineering Students*. Elsevier, 2005.

[58] Martin J. L. Turner. *Rocket and Spacecraft Propulsion*. Springer, third edition edition, 2009.

[59] Howard Curtis. *Orbital Mechanics for Engineering Students*. Elsevier, 2005.

[60] Jae-Woo Lee, Young-Ki Lee, Yung-Hwan Byun, and Ho-Yon Hwang. Design of Space Launch Vehicle Using Numerical Optimization and Inverse Method. *Journal of Spacecraft and Rockets*, 38(2):212–218, March 2001.

[61] Amer Farhan Rafique, Linshu He, Ali Kamran, and Qasim Zeeshan. Hyper Heuristic Approach for Design and Optimization of Satellite Launch Vehicle. *Chinese Journal of Aeronautics*, 24(2):150–163, April 2011.

[62] Mathieu Balesdent, Nicolas Bérend, Philippe Dépincé, and Abdelhamid Chriette. Multidisciplinary Design Optimization of Multi-Stage Launch Vehicle using Flight Phases Decomposition. *International Journal for Simulation and Multidisciplinary Design Optimization*, 4(3-4):117–125, February 2012.

[63] Douglas J. Bayley, Roy J. Hartfield, John E. Burkhalter, and Rhonald M. Jenkins. Design Optimization of a Space Launch Vehicle Using a Genetic Algorithm. *Journal of Spacecraft and Rockets*, 45(4):733–740, July 2008.

[64] L. Ridolfi, M. Pontani, and P. Teofilatto. Effect of different flight conditions at the release of a small spacecraft from a high performance aircraft. *Acta Astronautica*, 66(5-6):665–673, March 2010.

[65] J Roshanian and Z Keshavarz. Multidisciplinary design optimization applied to a sounding rocket. *Journal Indian Institute*, pages 363–375, 2006.

[66] Qasim Zeeshan, Dong Yunfeng, Khurram Nisar, Ali Kamran, and Amer Rafique. Multidisciplinary Design and Optimization of Multistage Ground-launched Boost Phase Interceptor Using Hybrid Search Algorithm. *Chinese Journal of Aeronautics*, 23(2):170–178, April 2010.

[67] S N Maitra. Constant thrust programming for a multistage rocket flown in vacuum with a given initial T/W. 8(October):373–385, 1985.

[68] GA AIAA Space 2001 Conference and Exposition Albuquerque , New Mexico. *AIAA 2001-4542 A Comparison of Modern and Historic Mass Estimating Relationships on a Two-Stage to Orbit Launch Vehicle* , 2001.

[69] Mauro Pontani and Paolo Teofilatto. Acta Astronautica Simple method for performance evaluation of multistage rockets. *Acta Astronautica*, pages 1–12, 2013.

[70] V Adimurthy and Vikram Sarabhai. Launch Vehicle Trajectory Optimization . *Acta Astronautica*, 15(11):845–850, 1987.

[71] Shashi Kant Shrivastava. Determination of optimal trajectory under design constraints for a satellite launch vehicles. *Acta Astronautica*, 3(September):333–347, 1976.

[72] Donald J Estep, Dewey H Hodges, and Michael Warner. The solution of a launch vehicle trajectory problem by an adaptive finite-element method. *Computer Methods in Applied Mechanics and Engineering*, 190:4677–4690, 2001.

[73] NASA. Optimum Rocket Trajectories. 27(8):955–961, 1956.

[74] A Miele. Rocket Flight in a Resisting Medium I. *Journal of Optimization Theory and applications*, (2).

[75] Glen J. Culler and Burton D. Fried. Universal Gravity Turn Trajectories. *Journal of Applied Physics*, 28(6):672, 1957.

[76] B D Fried, J M Richardson, and D F Lawden. General Formulation of Powered Flight Trajectory Optimization Problems. *Journal applied Physics*, (v):1203–1209, 1958.

[77] G E Dorrington. Gravity-Turn Trajectories. 37(4):543–544, 1990.

[78] Mathieu Balesdent. *OPTIMISATION MULTIDISCIPLINAIRE DE LANCEURS (Multidisciplinary Design Optimization of Launch Vehicles).* PhD thesis, École Centrale de Nantes, 2011.

[79] T Miele, A and Wang. Multiple-Subarc Gradient-Restoration Algorithm, Part 2: Application to a Multistage Launch Vehicle Design. *Journal of Optimization Theory and Applications*, 116(1):19–39, 2003.

Appendix A

Nose Cone Geometries

A.1 Nose Cone Geometries

There are several rocket nose cones, for this study four were considered: Ogive, Power, Ellipse and Haack [39]. As explained previously in chapter 4, the nose cones are added as extra volume to the last stage, resulting as fairing Volume. This volume is considered part of the total volume of the last stage.

A.1.1 Ogive

In the rocketry model, the most common ogive shape used is the tangent ogive, which is formed by the radius of curvature of the circle ρ_t

$$\rho_t = \frac{R^2 + L^2}{2R} \tag{A.1}$$

When the radius of curvature ρ is superior to ρ_t, the resulting nose cone has an angle at the joint between the nose cone and body tube, and is called a secant ogive. At the limit the secant ogive becomes a conical nose cone.

The parameter value k is the ratio of radius of curvature of a corresponding tangent ogive ρ_t to the radius of curvature of the nose cone ρ:

$$k = \frac{\rho_t}{\rho} \tag{A.2}$$

k takes values from zero to one, where k = 1 produces a tangent ogive and k = 0 produces a conical nose cone (infinite radius of curvature).

The radius of curvature is

$$\rho^2 = \frac{(L^2 + R^2) \cdot (((2-k)L)^2 + (kR)^2)}{4(kR)^2} \tag{A.3}$$

The radius will be

$$r(x) = \sqrt{\rho^2 - (\frac{L}{k-x}^{2})} - \sqrt{\rho^2 - (\frac{L}{k})^2} \tag{A.4}$$

In the following figure A.1, an example of a Power Nose cone is represented:

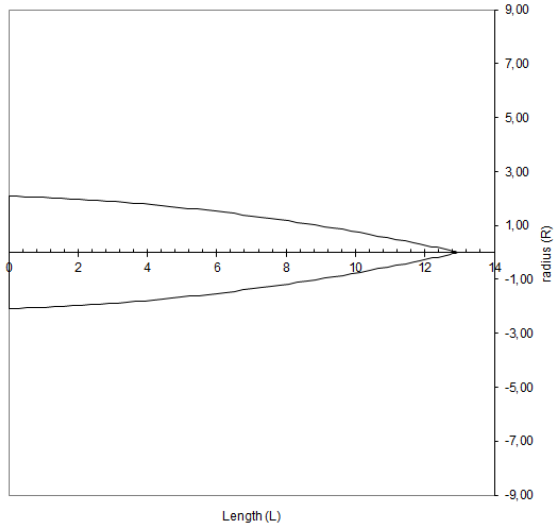

Figure A.1: Ogive

A.1.2 Power

$$r(x) = R(\frac{x}{L})^{\kappa} \tag{A.5}$$

The parameter value κ ranges between 0 and 1. There are 3 special cases: κ = 1 for a conical nose cone, κ = 0:75 for a 3/4 power nose cone and κ = 0.5 for a 1/2 Power Nose Cone or an ellipsoid. A blunt cylinder is formed when limit κ tends to 0.

In the following figure A.2, an example of a Power Nose cone is represented:

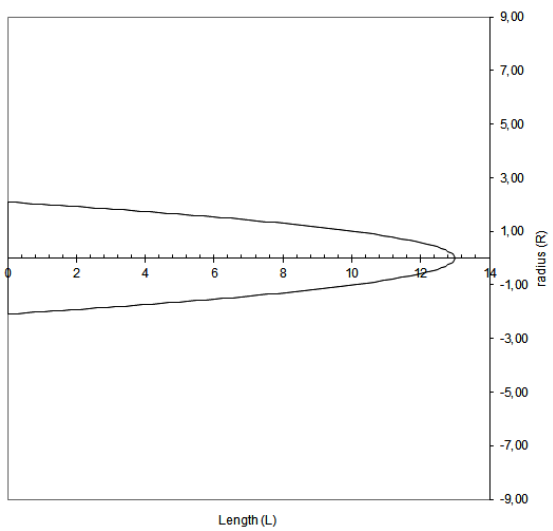

Figure A.2: Power

A.1.3 Ellipse

Ellipse or Elliptical Nose Cones have the shape of an ellipsoid. They are characterized by one major radius, L, and two other radius, R. Their profile is shaped like a half-ellipse, with major axis L and R. This is a common geometry in model rocketry, as Power also is.

The elliptical nose cone equation is:

$$r(x) = R\sqrt{1-(1-\frac{x}{L})^2} \tag{A.6}$$

When the radius R and L are equal, that corresponds to a half-sphere.

The figure A.3 is an example of an ellipse nose cone:

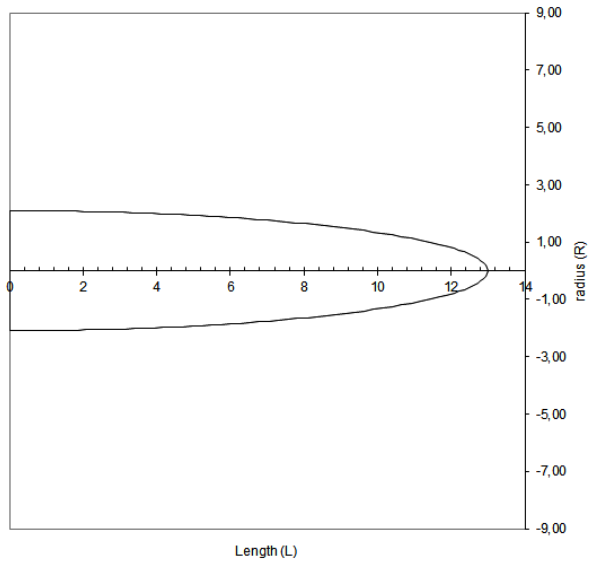

Figure A.3: Ellipse

A.1.4 Haack

The Haack series was mathematically designed to minimize the pressure Drag. They are divided in two shapes, the LV-Haack shape, this means with length-volume relation and the LD-Haack with length-diameter relation or Von Kárman shape. The parameters defining the dimensions of the nose cone are its length and radius.

The equation for the series is:

$$r(x) = \frac{R}{\sqrt{\pi}} \cdot \sqrt{\theta - \frac{1}{2} \cdot sin(2\theta) + k \cdot sin^3\theta} \tag{A.7}$$

Where:

$$\theta = cos^{-1} \cdot (1 - \frac{2x}{L}) \tag{A.8}$$

Where the parameter value k = 0 produces the Von Kárman of LD-Haack shape and k = 1/3 produces the LV-Haack shape. The value selected for k was 0.

The figure A.4 is an example of a Von Kárman - Haack series nose cone:

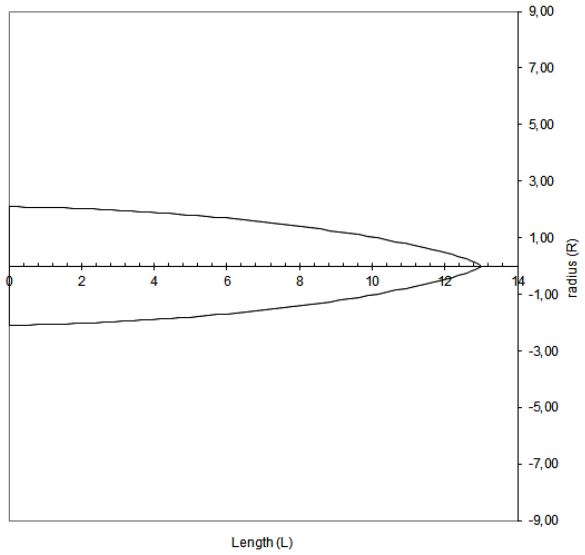

Figure A.4: Haack

Appendix B

Propellant properties

In the following table B.1 are presented some important properties of the propellants selected for the tool, such as the Oxidizer to Fuel ratio and the specific masses of the propellants. This values were used in the Mass and Volume models providing more realistic results in those fields.

Propellant	Isp	OF	$\rho_{oxidizer}$	ρ_{fuel}
LOX/H2	462	3.8	1142	71
LOX/Hydrazine	363	1.2	1142	1010
LOX/RP1	347	2.27	1142	810
Nitrogen Tetroxide/RP1	328	3.51	1440	810
Nitrogen Tetroxide/HTPB	297	3.17	1440	1810
LOX/HTPB	317	2.04	1142	1810
F2/H2	441	4.26	1509	71
Nitrogen Tetroxide/MMH	318	1	1440	878
Nitrogen Tetroxide/UDMH	313	1.75	1440	789
Nitrogen Tetroxide/Hydrazine	309	2.21	1440	1010
HTPB/AP	265	-	1800	-
DB-HMX/AP	260	-	1854	-

Table B.1: Propellant Specifications